

Chapter IV

The Construction of AMS-02

AMS is scheduled to be installed on the Space Station in March 2004 for a period of three to five years. (Figure 26) AMS physicists are involved in all parts of the AMS-02 design and construction (see also Figure 4), as shown in the current management structure of AMS-02 of Table 7.

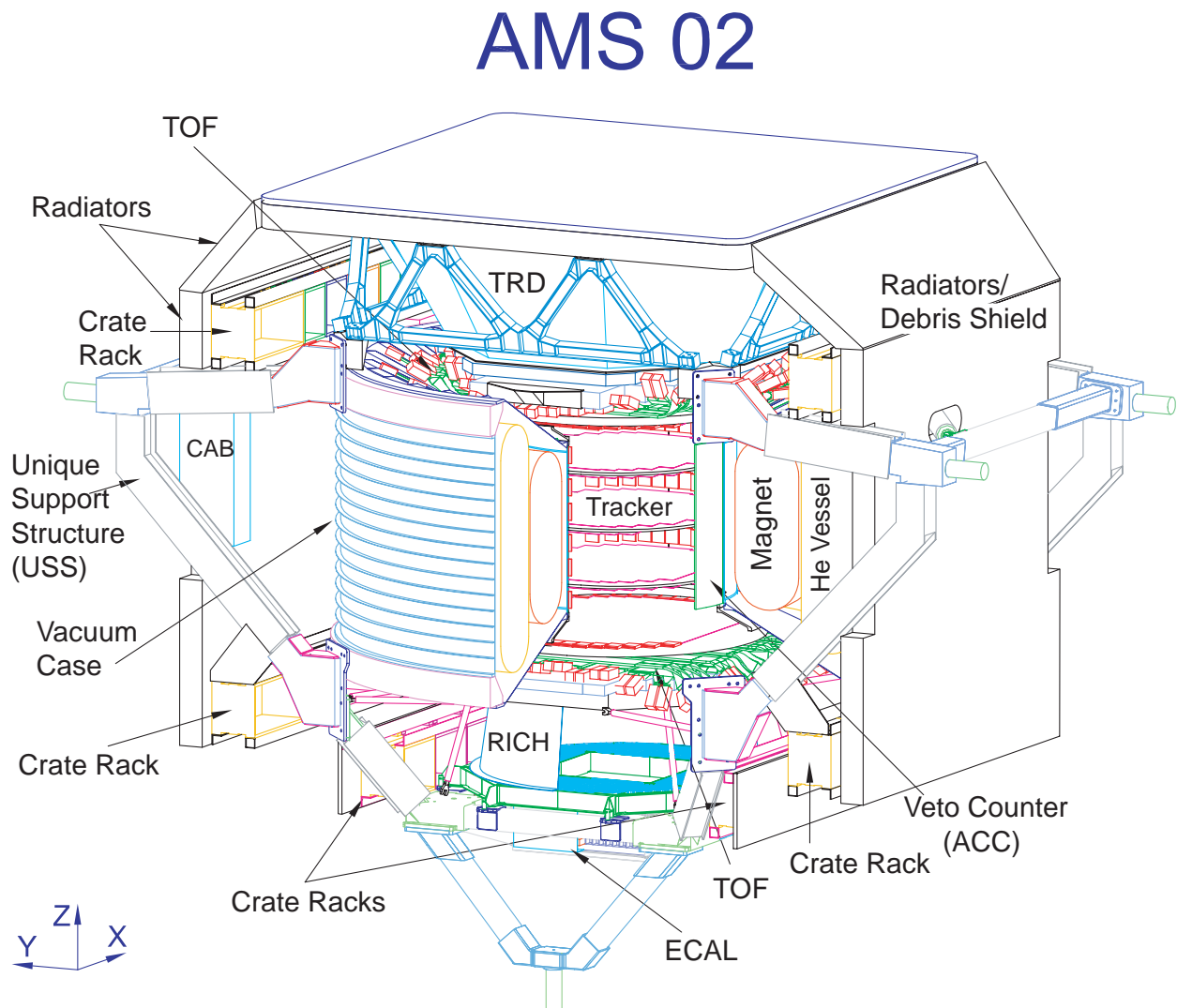


Figure 26 : AMS-02 Experiment as it will appear on the ISS. In addition to the detector elements of Figure 4, this figure shows the structural interface (USS) which connects the detector to the shuttle and to the ISS, the thermal radiators, debris shields, the electronics crate racks and the location of the Cryomagnet Avionics Box (CAB).

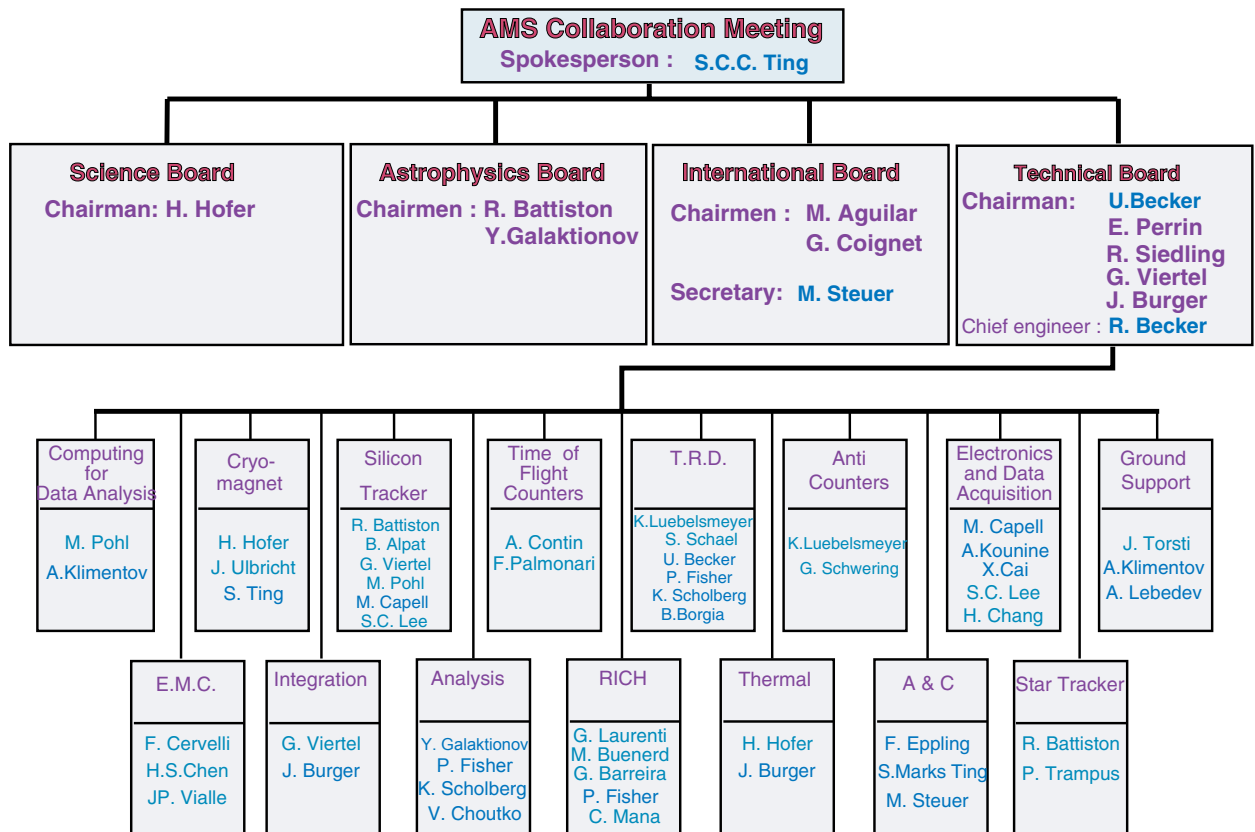


Table 7 : AMS-02 Management structure and key coordinators :

As will be described in the following sections, the construction of the detector is progressing well. Because this is the only high energy physics experiment on the Space Station, NASA is following the progress of AMS with detailed reviews concerning the design and construction, safety and ground operations to ensure the detector can be launched in March 2004 (see Tables 8 and 9).

The magnet will be completed at the end of 2002. The detectors will be completed at the beginning of 2002 and we have arranged for extensive beam tests in the later half of 2002. Integration and assembly of the detectors into the magnet and support structure will occur in March 2003 and the entire system will be tested again in the CERN accelerator beams in the summer of 2003, followed by an extensive thermal vacuum test at NASA Johnson Space Center before delivery to Kennedy Space Center at the end of 2003.

It should be noted that the major construction of AMS-02 is being done in Europe and Asia, particularly in Taiwan for the electronics (see Figure 1 and the electronics section VIII). The graph below shows the participation of some of the senior AMS-02 physicists from different European Institutes.



European Participation in AMS-02 construction.

I. The Cryomagnet

1) Design and construction of the Cryomagnet

The purpose of the superconducting magnet is to extend the energy range of measurements of particles and nuclei to multi-TeV region. The AMS-02 magnet design is under the overall responsibility of H. Hofer of ETH, Zürich, supported by J. Ulbricht, S. Ting and others. The magnet design was based on the following technical considerations :

- (i) Experience in designing and manufacturing the AMS-01 magnet which was 10 times safer than stress limits allowed (see Chapter II, Table 5 : "Report of stress test on the AMS-01 magnet").
- (ii) The result of many years (since September 1997) of intensive R&D collaboration between ETH and the R&D group of Oxford Instruments Ltd. to design a magnet with the following properties :
 - a) Identical field configurations to the AMS-01 magnet to maintain mechanical stability and follow NASA safety standards, as shown in Figure 27.
 - b) Minimized heat loss (~100 mW) and minimized quench probability.

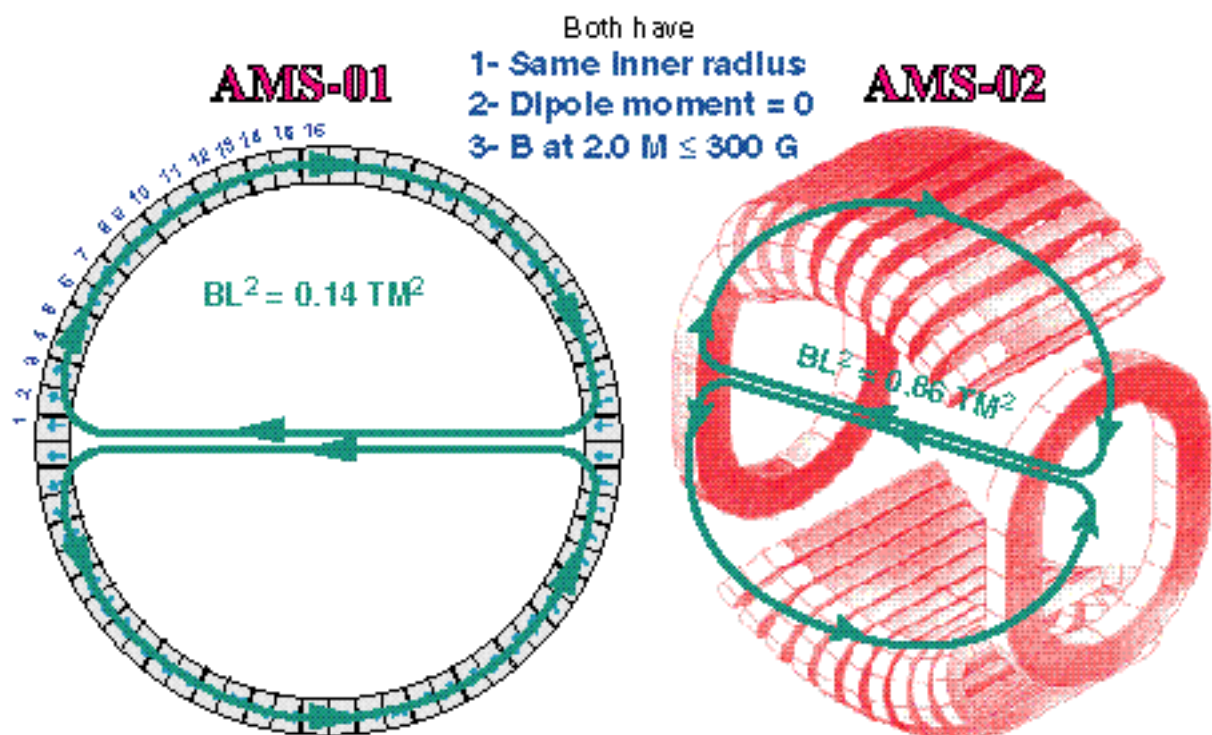


Figure 27 : Identical magnet configuration between AMS-01 and AMS-02 magnets

- (iii) We have chosen to have the magnet built by experts from the Oxford Instruments R&D group, who have an excellent record to produce highly reliable magnets in persistent mode without quench. This group has produced the 8 OSCAR magnets (2.36 Tesla) used in cyclotrons in Japan and England and which have operated for close to 30 years without any quench. This group also built the CLEO magnet at CORNELL and the CLAS Torus at

Jefferson Laboratory and the KLOE magnet in Frascati. All are large, high-field, special-purpose magnets which have operated for years without quench.

To ensure that these experts are able to devote all their efforts to the construction of the AMS-02 magnet, the Swiss Government has supported a new company : Space Cryomagnetics Ltd., entirely staffed by the experts of the Oxford Instruments R&D group. Oxford Instruments Ltd. has given their strong logistic support to this effort.

- (iv) Most importantly, we are using the new aluminum-stabilized conductor developed and mass-produced by the ETH-Hofer magnet group. Based on test results, this conductor will reduce the quench probability by a factor of 2000. This new type of aluminum-stabilized conductor is now widely used as shown in Figure 28.

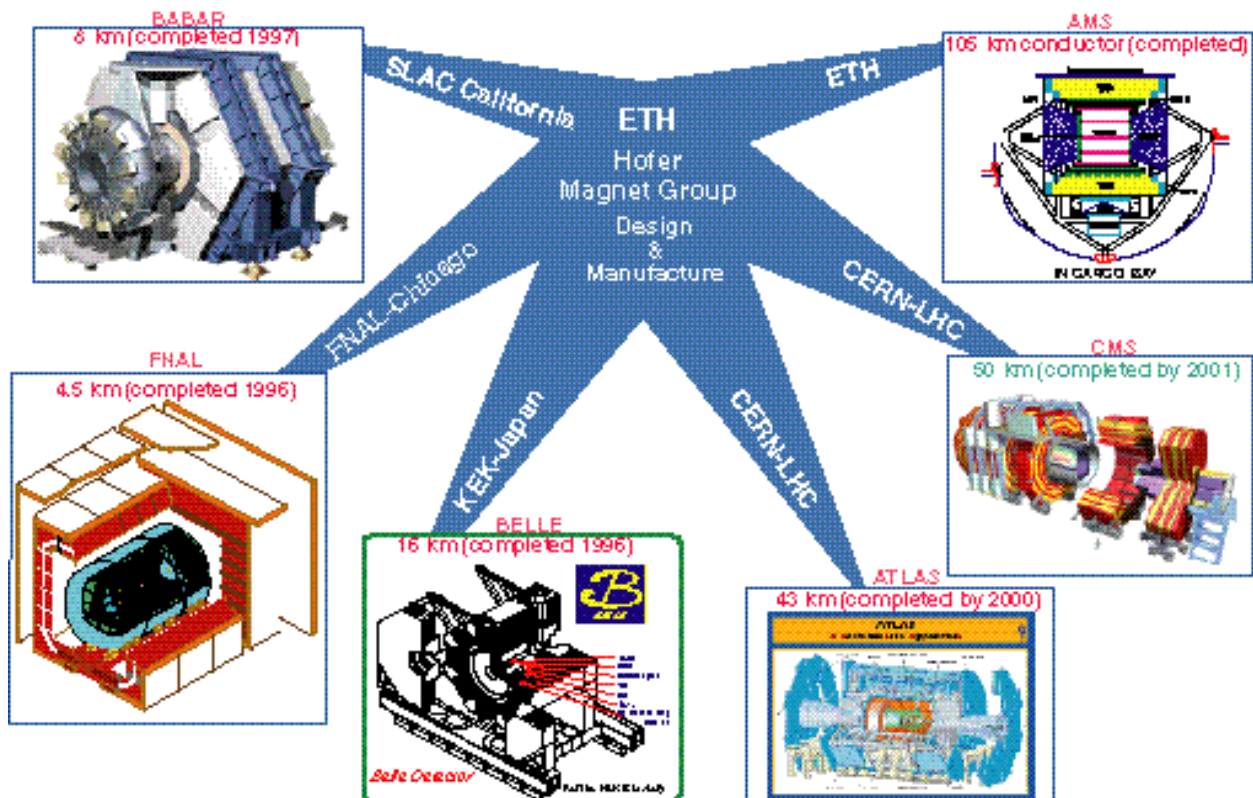


Figure 28 : New type of aluminum-stabilized conductor used for HEP detectors

The AMS-02 cryomagnet is now under construction. Two identical magnets will be built. One will be the flight magnet (see Figure 29); the second one will be used for space qualification tests. The magnet will have no magnetic field during the shuttle launch and landing and so there will be no force among the coils, hence for the test magnet the coils will be replaced by mass equivalents.

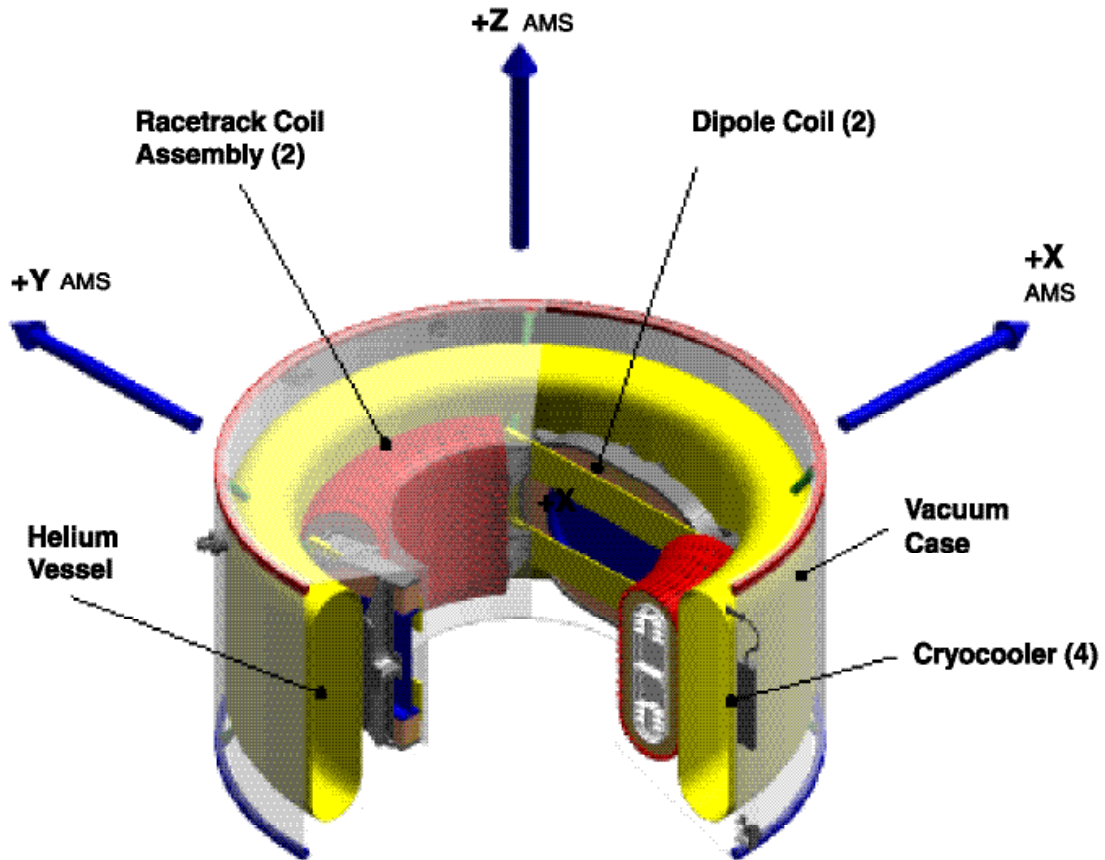


Figure 29 : AMS-02 superconducting magnet layout.

The magnet weighs 2.1 tons, with an outside diameter of 2.7 m and a height of 1.5 m. It is designed to operate at zero gravity and withstand 10 to 12 g on launch and landing. The two dipole coils and two arrays of race track coils will be cooled by 2500 liters of superfluid helium. Four 8-watt cryo-coolers will ensure a lifetime of three to five years in space.

Table 10 summarizes the sharing of responsibilities in the construction of the magnet.

Overall Responsibility	ETH-MIT
Cold Mass (Coil and Structure)	Space Cryomagnetics Ltd.
Aluminium-stabilized Conductor	ETH-Zürich, INFN Milano
Integrated Vacuum Vessel	NASA, Houston
	Lockheed Martin, Houston
Cryo Pumps	ETH-MIT with NASA-GSFC
Cryo Valves	WEKA, near Zürich
Electronics	MIT, Cambridge
Power Supply	Spain and CRISA
Mechanical Support	CSIST, Taiwan

Table 10 : AMS-02 Cryomagnet Responsibilities

Figure 30 shows the magnet geometry of the coils and Table 11 summarizes some of the cryomagnet parameters :

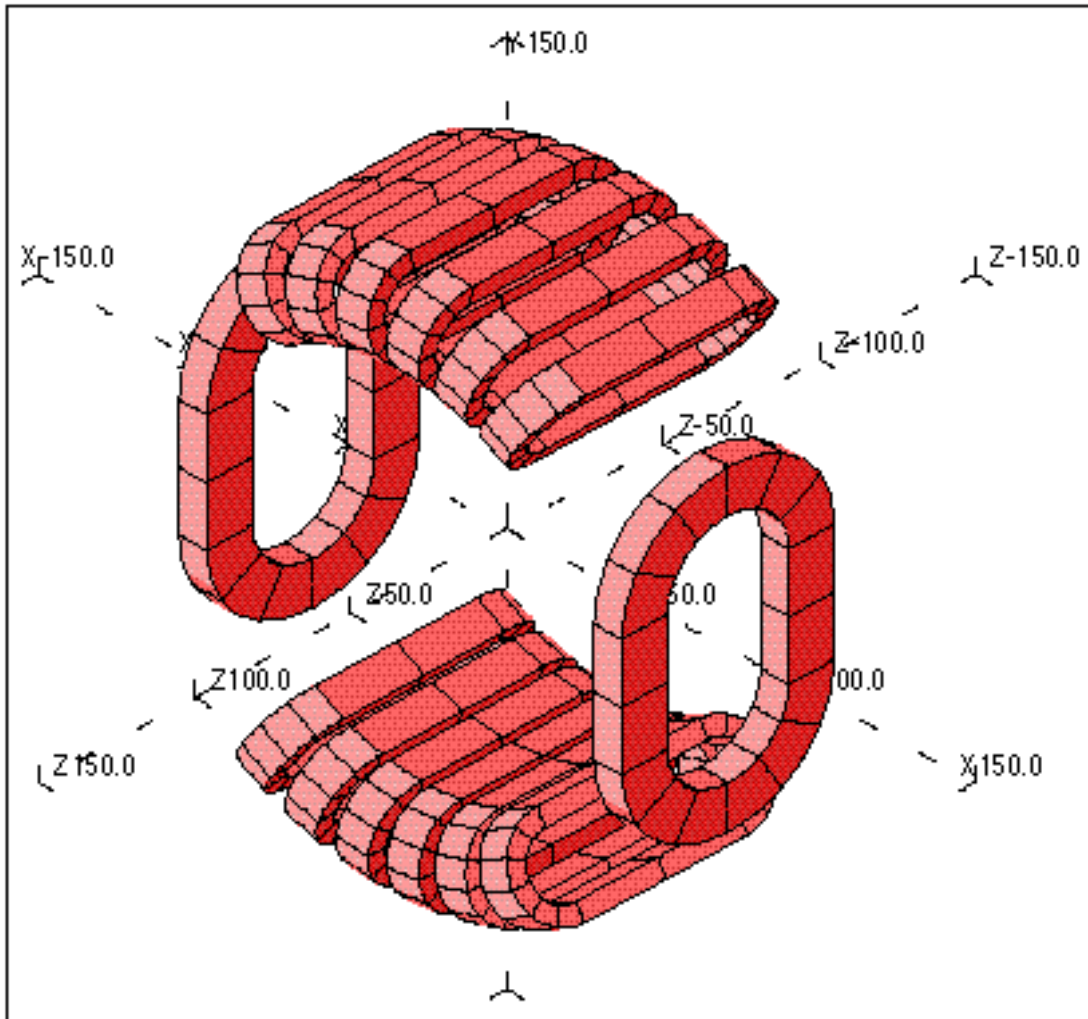


Figure 30 : Magnet geometry of the coils.

Parameters	
Central Magnetic Field $B_x(0,0)$ [T]	0.867
Dipole Bending Power [Tm^2]	0.862
Maximum Stray Magnetic Field at $R=2.3$ m [mT]	15.2
Maximum Stray Magnetic Field at $Y=2.3$ m [mT]	7.6
Maximum Stray Magnetic Field at $R=3.0$ m [mT]	3.9
Peak Magnetic Field on the Dipole Coils [T]	6.59
Peak Magnetic Field on the Racetrack Coils [T]	5.91
Maximum Torque [Nm]	0.272
Nominal Operating Magnet Current [A]	459
Stored Energy [MJ]	5.15
Nominal Magnet Inductance [H]	48.9

Table 11 : AMS-02 Cryomagnet parameters.

Figure 31 shows a cross-section of the aluminum-stabilized conductors developed by the ETH Hofer group. The current density in the superconductor is $2300\text{A}/\text{mm}^2$. The overall current density (including aluminum) is $157\text{ A}/\text{mm}^2$. All of the conductor (a total of a 105 km) has been produced.

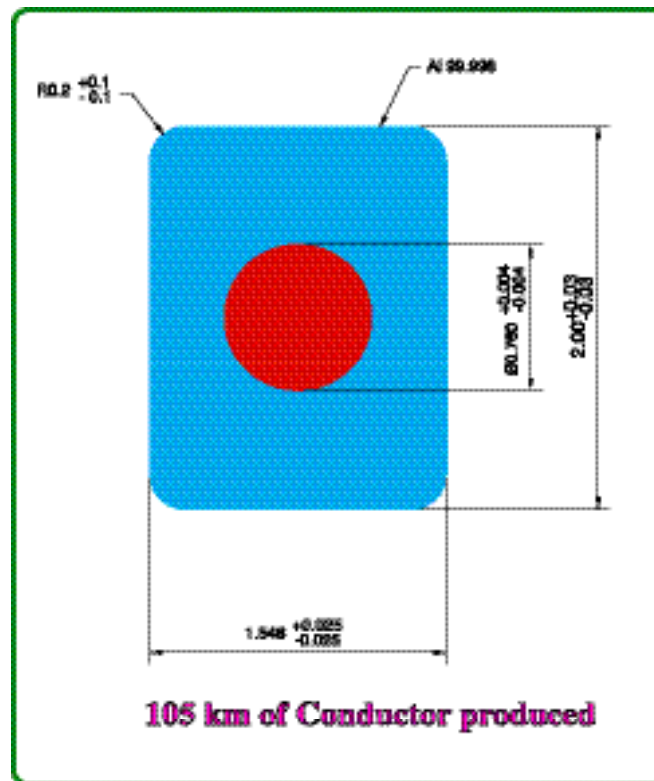


Figure 31 : Aluminum stabilized NbTi/copper composite conductor cross-section under the responsibility of ETH-Zürich and INFN Milano. Dimensions in mm.

Figure 32 shows the detailed mechanical design of the magnet system. Figure 33 is an isometric view of the magnet system, Figure 34 shows the arrangement of the magnet vacuum case and helium tank and Figure 35 shows the detail of the helium vessel. Two are being built : one for the test magnet and the other for the flight magnet. Figure 36 shows the detail of the vacuum tank. Again, two vacuum tanks are being built : one for the test magnet, one for the flight magnet. The magnet design and construction procedures are the result of many years of efforts by Oxford Instruments Ltd., Space Cryomagnetics Ltd., ETH-MIT, NASA and Lockheed Martin Space Mission Systems & Services. It has successfully passed the first NASA Safety Review.

Extensive test procedures are being carried out in parallel with the construction. Four full-size race-track test coils are under construction to verify the cooling and quench behavior, quench protection and mechanical behavior at large over current and other safety-related issues. One race-track test coil is shown in Figure 37. Figure 38 shows a scaled-down super-fluid helium dewar fabricated to test the rate of overboard venting should the helium tank be punctured during the launch or ascent. This test is important to avoid possible over-pressure in the shuttle bay.

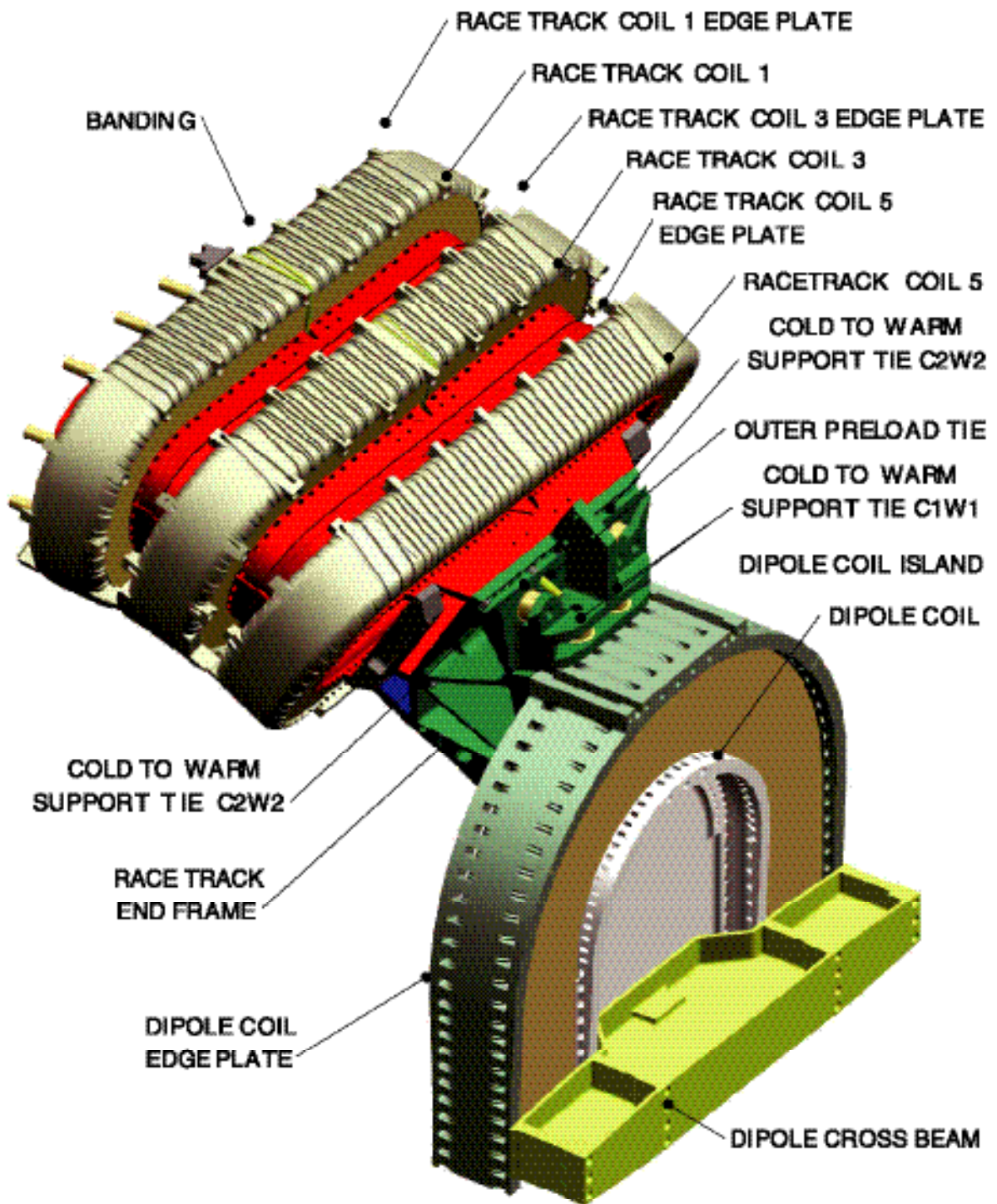


Figure 33 : An isometric view of 1/4 of the magnet system.

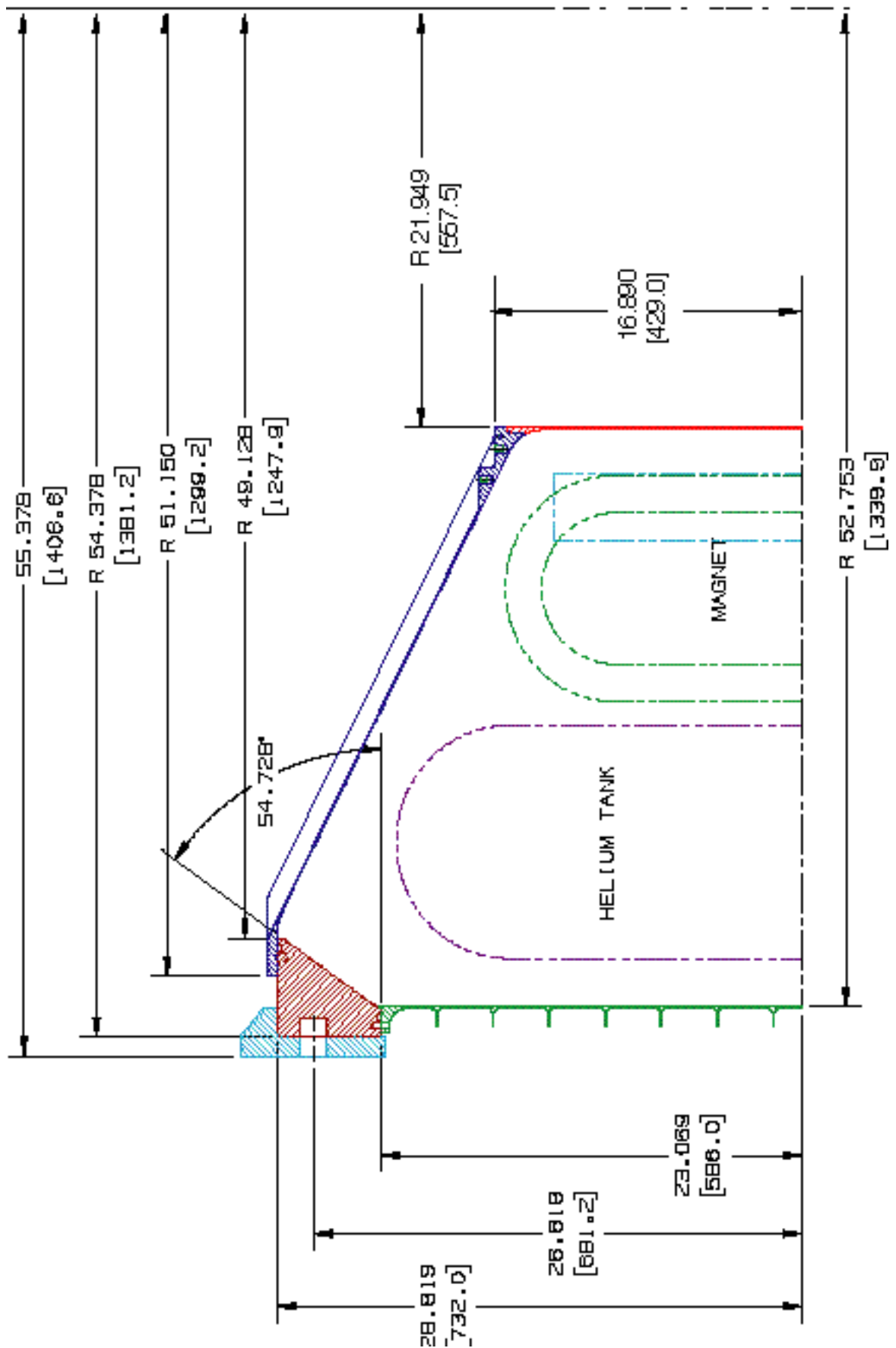


Figure 34 : Magnet Vacuum case and Helium Tank Assembly

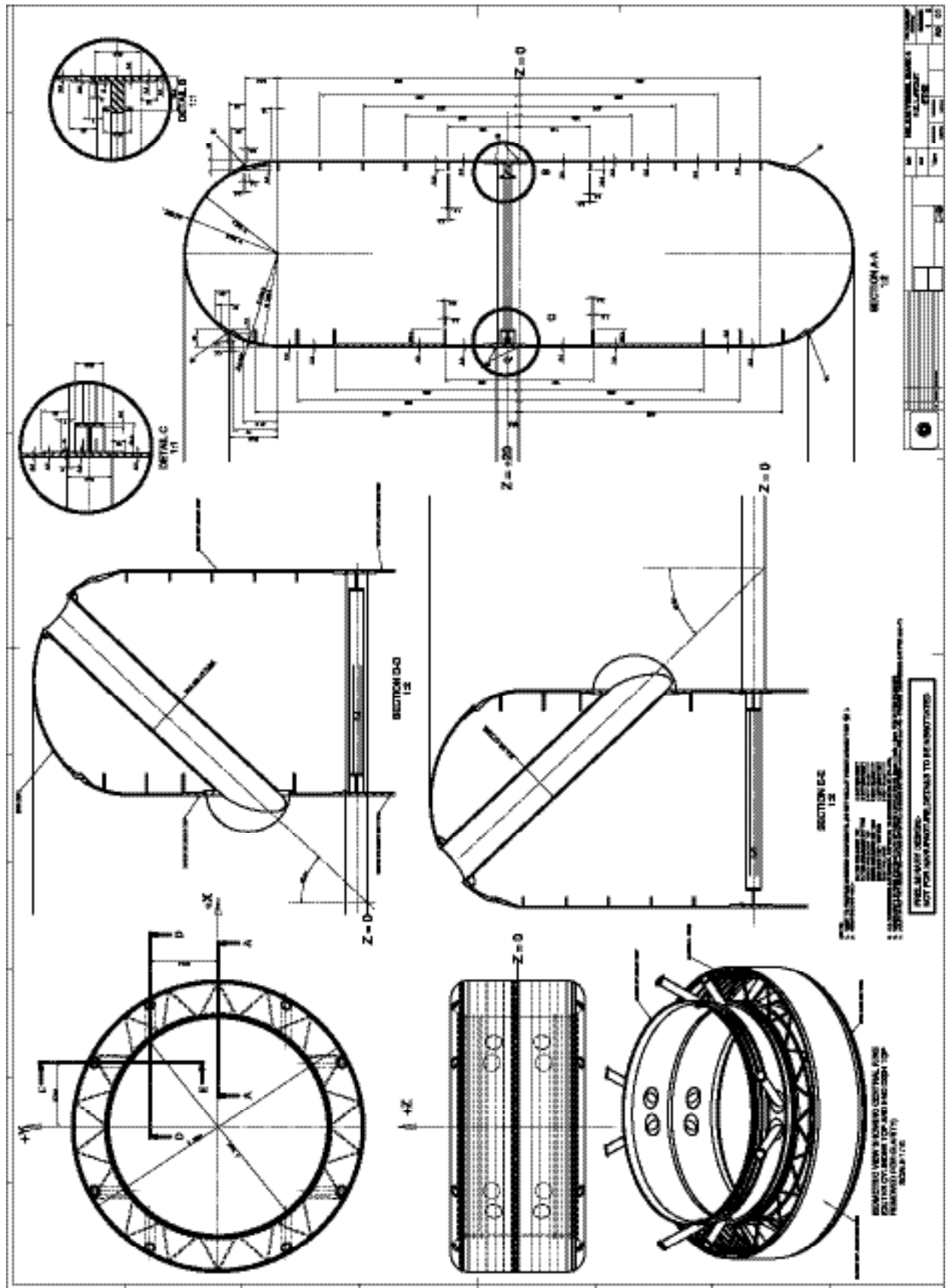


Figure 35 :Detail of Helium Vessel. Two identical helium vessels are being Built: one for the safety tests, the other for the flight.

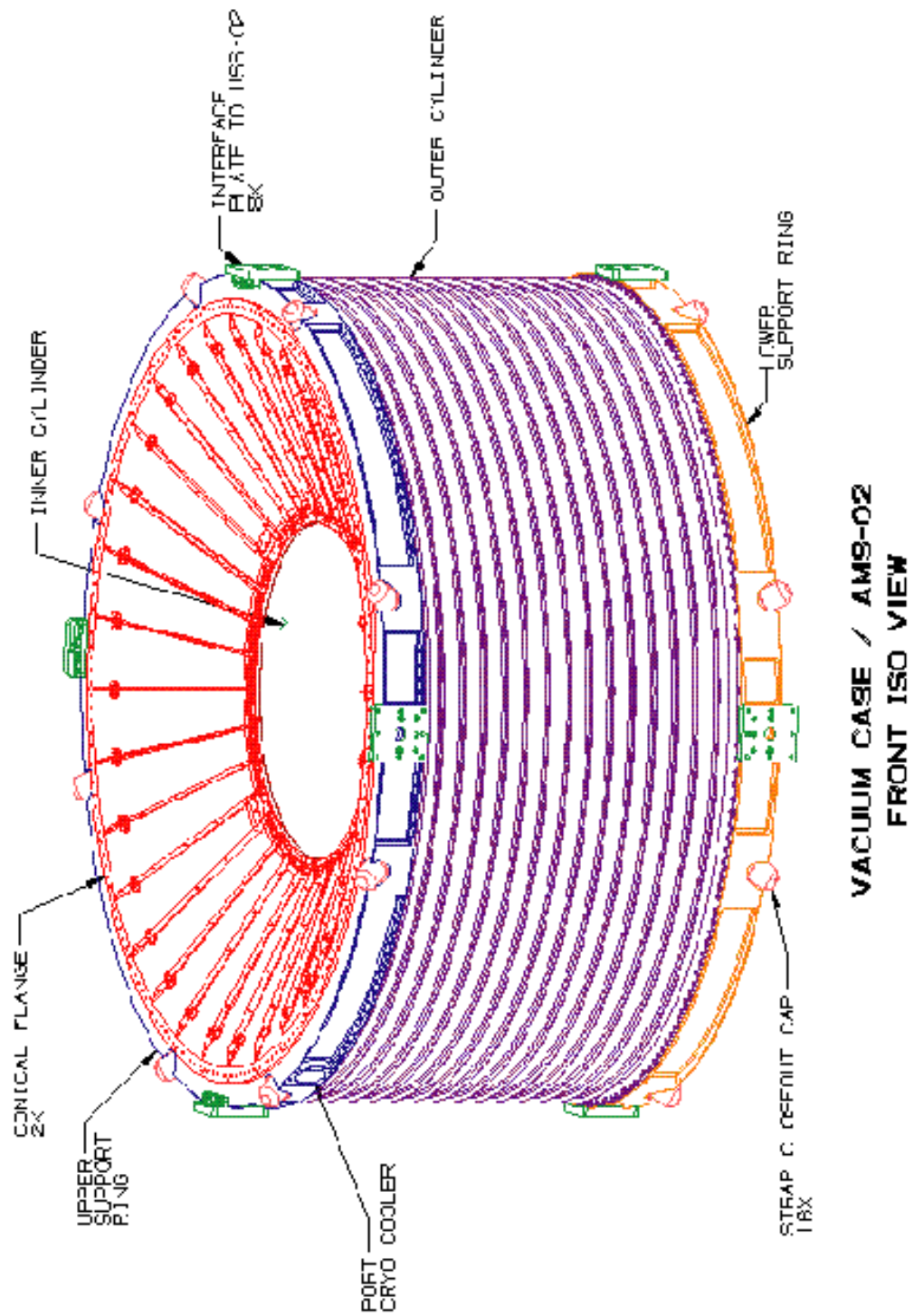
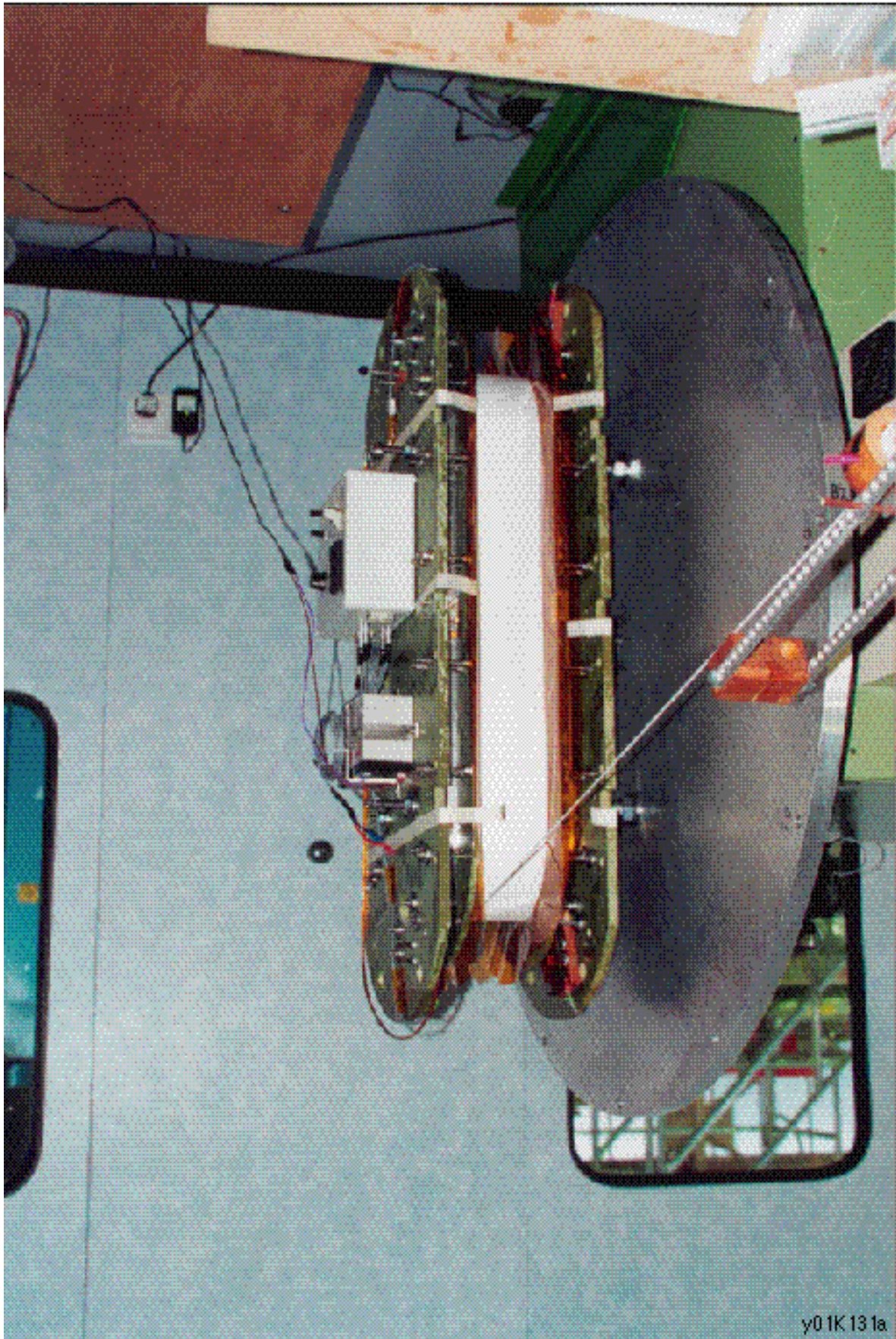


Figure 36 : Detail of the Vacuum Tank. Two are being built : one for the flight, one for safety tests.



y01K13 1a

Figure 37 : One of the four full-size race-track coils under construction.

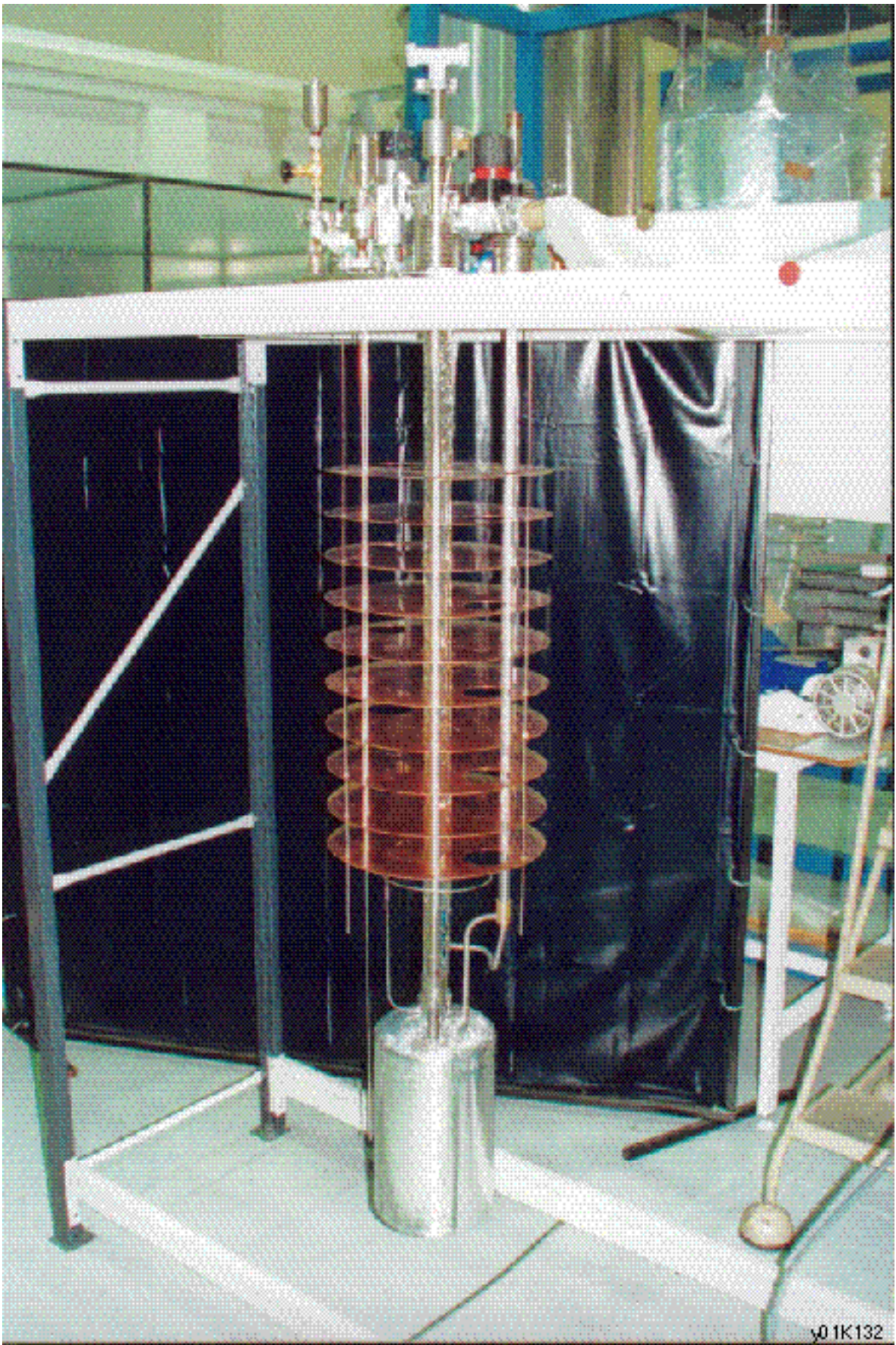


Figure 38 : Test Assembly of Super-fluid Helium Dewar

2) The Cryogenics System

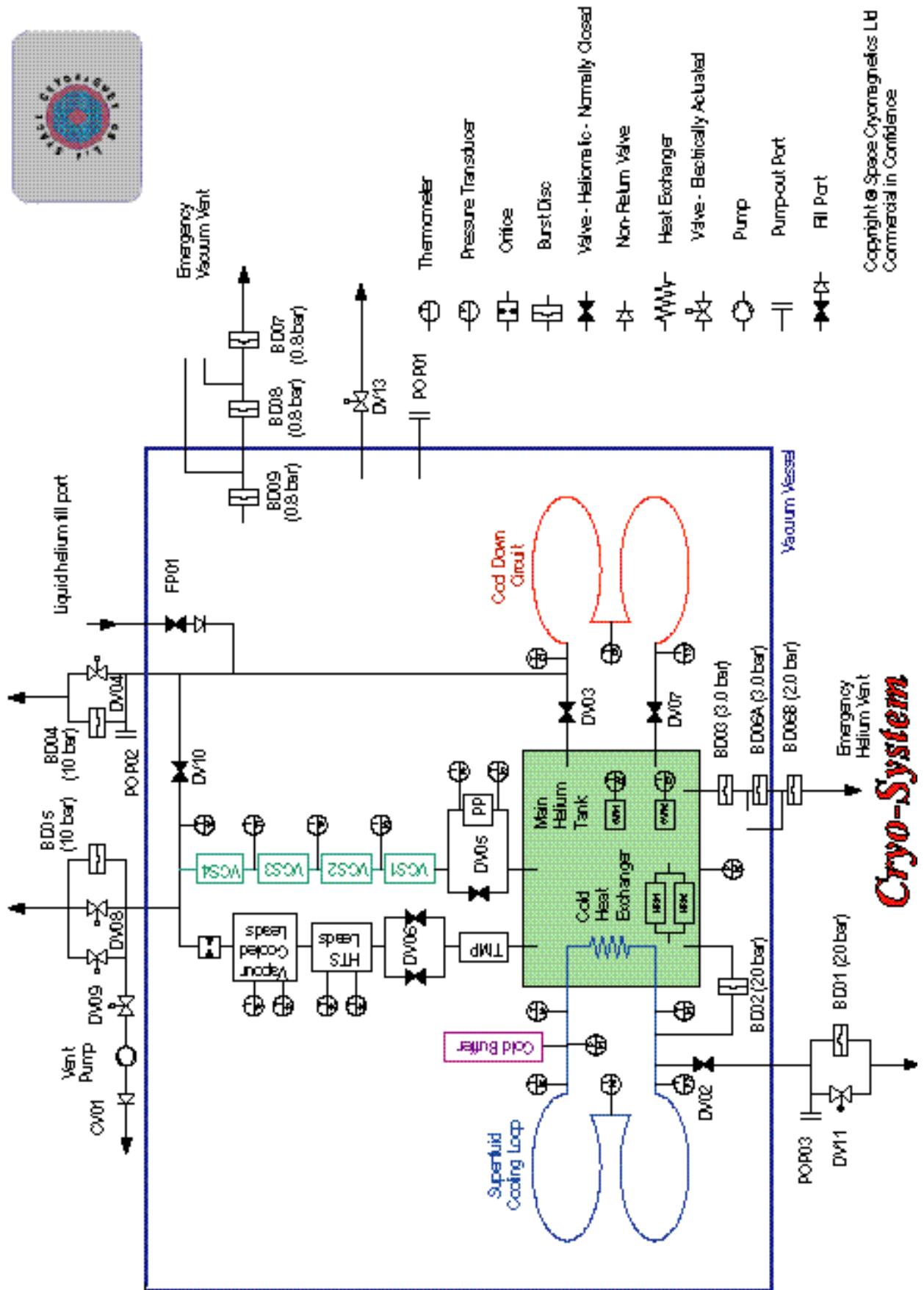
Figure 39 shows a schematic of the AMS-02 Cryogenics-system. Before use the system is cooled down from room temperature to 80K by cold helium gas passing through the Cool Down Circuit, into the Main Helium Tank and out through the Vapor-Cooled Shields (VCS1, VCS2, VCS3, and VCS4).

Pressure and cleanliness is maintained in the Superfluid Cooling Loop by a separate supply of dry helium gas. Then liquid helium is introduced, first to purge the transfer line of gas, then to fill the Main Helium Tank and Cool Down Circuit, venting gas through the Vapor-Cooled Shields (VCS1, VCS2, VCS3, and VCS4). The Superfluid Cooling Loop, which keeps the magnet coils cold, is closed after being pressurized to 9.8 bar absolute at 4.2 K. The helium in the main tank is cooled down to superfluid temperature by pumping on the output line while continuing to fill. As the Main Helium Tank is filled, the helium in the Superfluid Cooling Loop also goes superfluid and reaches 1.85 K and 3 bar absolute.

The cold helium is thermally insulated by the vacuum vessel and layers of shielding which are cooled by the cold vapor of the helium as it boils off. In addition, four cryocoolers (see Figure 29) cool the outermost vapor cooled shield to minimize the loss of helium. On the ground, the system runs stably with a vacuum pump on the outlet. The system is sealed just before launch. The vent line is opened during ascent when the outside pressure drops below the pressure in the Main Helium Tank.

After launch the cryocoolers are turned on and the vacuum vessel is opened to space. The system is designed to minimize helium loss in case of a quench in space. In case of quench, the pressure in the Superfluid Cooling Loop rises, but the helium expands into the Cold Buffer and not into the Main Helium Tank. Afterwards the coils are cooled by flowing superfluid helium from the Main Helium Tank through the Cool Down Circuit until the coils are cold enough for the Superfluid Cooling Loop to operate again.

We expect the system to operate normally, without quenches, for three to five years. Loss of insulating vacuum can occur only on the ground, at the beginning of launch and at the end of landing. The vessel is designed and tested to prevent overpressure in the shuttle bay from boiling helium in case of vacuum loss during launch or landing.



- Thermometer
- Pressure Transducer
- Orifice
- Burst Disc
- Valve - Helionetic - Normally Closed
- Non-Return Valve
- Heat Exchanger
- Valve - Electrically Actuated
- Pump
- Pumpout Port
- Fill Port

Copyright © Space Cryogenics Ltd
Commercial in Confidence

Figure 39 : Design of the AMS-02 Cryo-System (DV : digital valve; HTS : high temperature superconductor; TMP : Thermo-mechanical pump; PP : poros plug).

3) The Cryomagnet Avionics

The electronics to power, monitor and control the magnet on-orbit will be primarily housed inside the Cryomagnet Avionics Box (CAB). As illustrated in Figure 40, the CAB contains four subsystems :

- the Cryomagnet Controller and Signal Conditioner (CCSC) which includes the precision current shunt and flywheel energy dump diodes mounted outside the CAB.
- the Cryomagnet Current Source (CCS),
- the Cryomagnet Self Protection (CSP) and
- Power Switches.

Figure 40 also shows the major electrical features of the magnet which include the super conducting coils with a load of zero Ohms and an inductance of 48 Henries, the mechanical lead disconnects, the quench heaters, the persistent switch, warm and cryogenic valves and associated temperature, pressure and voltage sensors. Additional sensors are located within the CAB itself.

Operationally, the magnet will be launched cold but unpowered and powered up only after installation on the ISS. Whenever the experiment is powered the CCSC will continuously monitor the magnet state and relay these readings through the AMS CAN bus housekeeping network. On orbit the information will then flow to AMS computer inside the ISS and to the central computers on the ground. Altogether about 150 values are monitored including 23 prime and 23 redundant cryogenic temperature measurements based on CERNOX sensors, which cover ranges from 1.4 to 400 K with accuracies down to 1 mK. These exacting measurements allow the proper functioning of the cryogenic plumbing to be accurately controlled. Commands follow the reverse path to reach the CCSC, which then initiates the appropriate action within the CAB or the magnet.

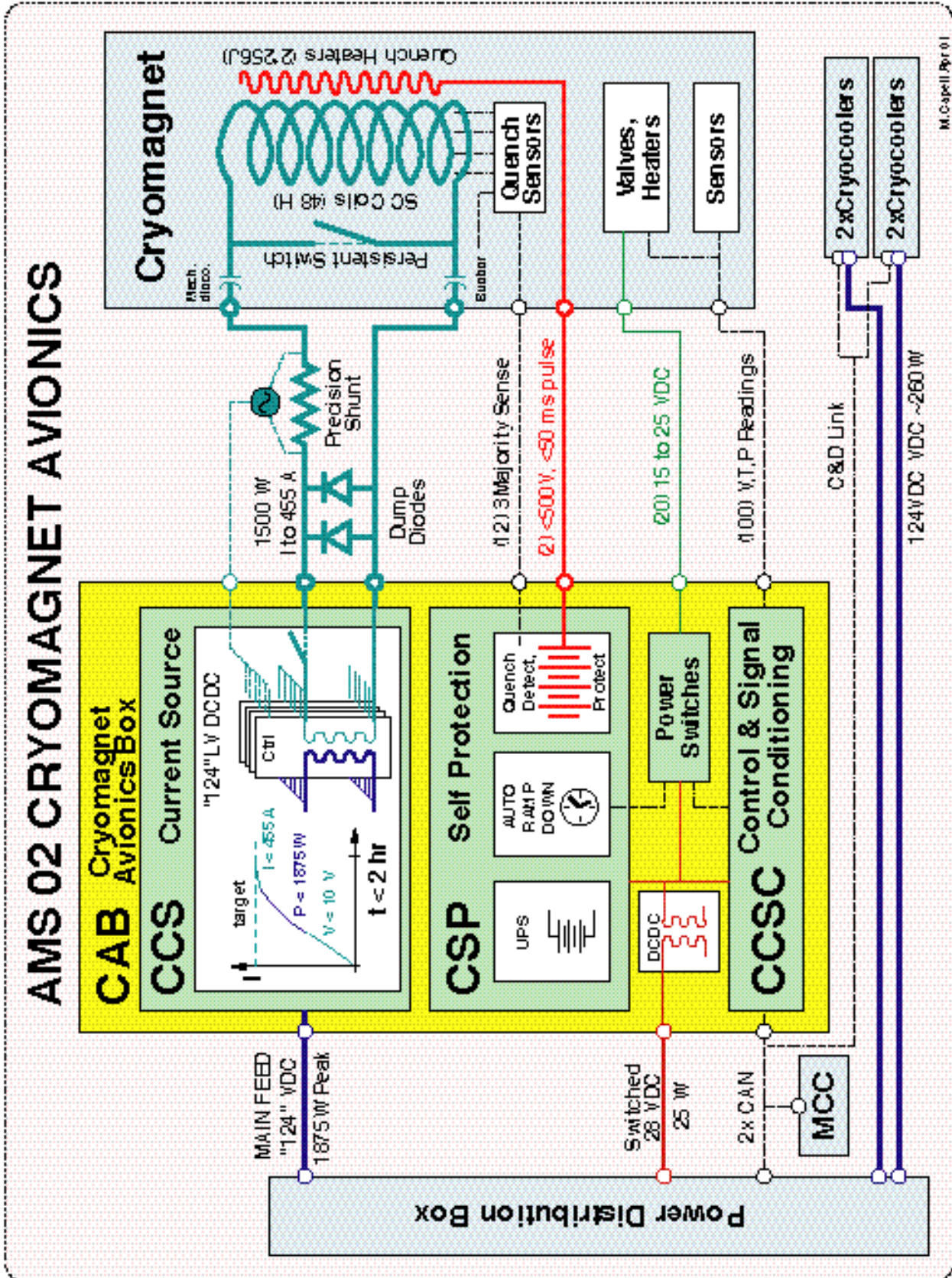


Figure 40 : AMS-02 Cryomagnet Avionics

The magnet is charged by the CCS. Before operations begin various checks are performed to ensure, for example, that the magnet coil circuit within the cold volume is superconducting. The complete charging operation then consists of five phases: preparation, output voltage limited charging, power limited charging, current limited charging and disconnection. To prepare the magnet for charging and the mechanical lead disconnects for cooling and then closing, the superconducting persistent switch is "opened" by heating it into the normal state. Then power is drawn directly from the ISS 124 VDC main feed and converted to a maximum of 10 VDC by six DC-DC converters in parallel. The resulting current flows through the precision shunt, magnet bus bars and through the magnet coils. In the third phase the power drawn from the ISS is limited to 1875W and the current in the coils continues to increase while the output voltage drops. Then the target coil current, nominally 455A, as monitored by the precision shunt is smoothly approached. After the target current is reached the system is allowed to settle and the persistent switch is allowed to cool and again become superconducting. The CCS is then shutdown and the magnet leads mechanically disconnected. In total the charging process is estimated to take less than two hours.

Ramping the magnet current down is less complicated. The CCS remains powered off, the magnet leads are cooled and connected and the persistent switch is again driven open. The current in the magnet coils then flows through the flywheel dump diodes which are mounted directly on the Unique Support Structure (USS). To dissipate the 5 MJ stored in the magnet is estimated to take less than 90 minutes.

The CSP has two primary functions: to automatically ramp down the magnet after a delay should services to the experiment be interrupted and to detect and protect the magnet should a quench occur.

When charged, the magnet current would continue to circulate indefinitely, even if the experiment was powered down or the command path to the experiment was broken. To obviate concerns arising from this, the CSP contains a battery backup and is connected to the controls necessary to monitor and perform the magnet ramp down described above. This "dead man" switch has an internal delay which can be set to allow interruptions of several hours without action, depending on experience with ISS operations.

Another concern is that if the magnet were to quench the entire stored energy would attempt to dissipate itself at the point in the circuit which had gone normal. This could lead to high temperatures and voltages at that point and to large stresses between the magnet coils and

supporting structure. To protect against this, the CSP monitors the voltages between the coils whenever the magnet is charged, where a non-zero voltage would indicate the onset of a quench. In this situation the CSP connects a capacitor bank to heaters located on each of the magnet coils. All of the coils are then driven normal and the energy dissipated evenly throughout the magnet. Similarly the CSP protects the bus bars and magnet leads against an over-temperature condition by monitoring these critical temperatures and initiating a magnet quench if needed. The requirements of this function are : the onset of a quench must be detected within 50 milliseconds and 256 Joules pulsed through either of the two heater chains within an additional 50 milliseconds. In addition this function should be active whenever the magnet has stored energy: when it is being charged, discharged during steady state running and during the possible several hour interval between service interruption and the onset of automatic ramp down.

It should be stressed that, owing to the advanced properties of the AMS superconductor and the cryogenics design, none of these conditions, including a spontaneous magnet quench, is anticipated to occur on orbit. However, should it ever happen, this design ensures that the magnet will not be damaged and that after re-cooling it can be recharged and the mission can proceed successfully. In any case, no hazard will be presented.

The fourth CAB subsystem, the power switches, allow the indirect operation of the various valves and heaters by the CCSC and the CSP. In addition the CAB contains several DC-DC converters to energize the CCSC and the CSP.

Owing to the amount of stored power and because the CCS within the CAB is connected directly to the ISS power bus, detailed analysis has been done to ensure proper grounding and isolation, both against possible breakdowns and against electromagnetic interference within the CAB, between the CAB and the rest of AMS, and between the CAB and the ISS.

The level of space qualification required for the CAB project is significantly more stringent than for the bulk of the electronics in AMS 02. From design and procurement through production and testing the CAB will use usual space quality techniques. The entire CAB has been designed to be single fault tolerant and certain critical blocks have been replicated to allow successful operation after multiple faults. For example, should one of the six primary DC-DC converters fail in the CCS, the remaining five are sufficient to reach full field. Even if a second converter were to fail, the field value could reach over 80 % of nominal. As another example, the target current is obtained by using the median result between three independent circuits which compare the voltage drop measured across the precision shunt to a reference voltage,

where each circuit is fed by an independently generated reference. Also, the control, signal condition blocks of the CCSC and the power switching are redundantly duplicated and cross strapped, with the primary and redundant sides being independently powered with dedicated converters and 28VDC feeds.

In the AMS collaboration, the CAB is part of the cryomagnet effort led by ETH, for which the prime contractor is Space Cryomagnetics. Overview of the magnet electronics is an MIT responsibility.

4) Cryo-magnet Schedule

The construction of the cryomagnet is on schedule with the assembly of the detector on the magnet (Figure 41) shown in Table 9. The major milestones accomplished are the following :

- 1) Vacuum case : is ordered
- 2) Helium vessel : is designed
- 3) Superconducting cables : 105 km are produced
- 4) Mechanical design : is completed and a prototype ordered
- 5) Special test coil : is under construction
- 6) Cryosystem : is designed, ready for verification tests
- 7) Cryomagnet avionics : is ready for pre-production.

At the same time, the test magnet will be going through extensive space qualification tests at NASA Johnson Space Center to ensure that the vacuum tank and the helium vessel can withstand space environment.

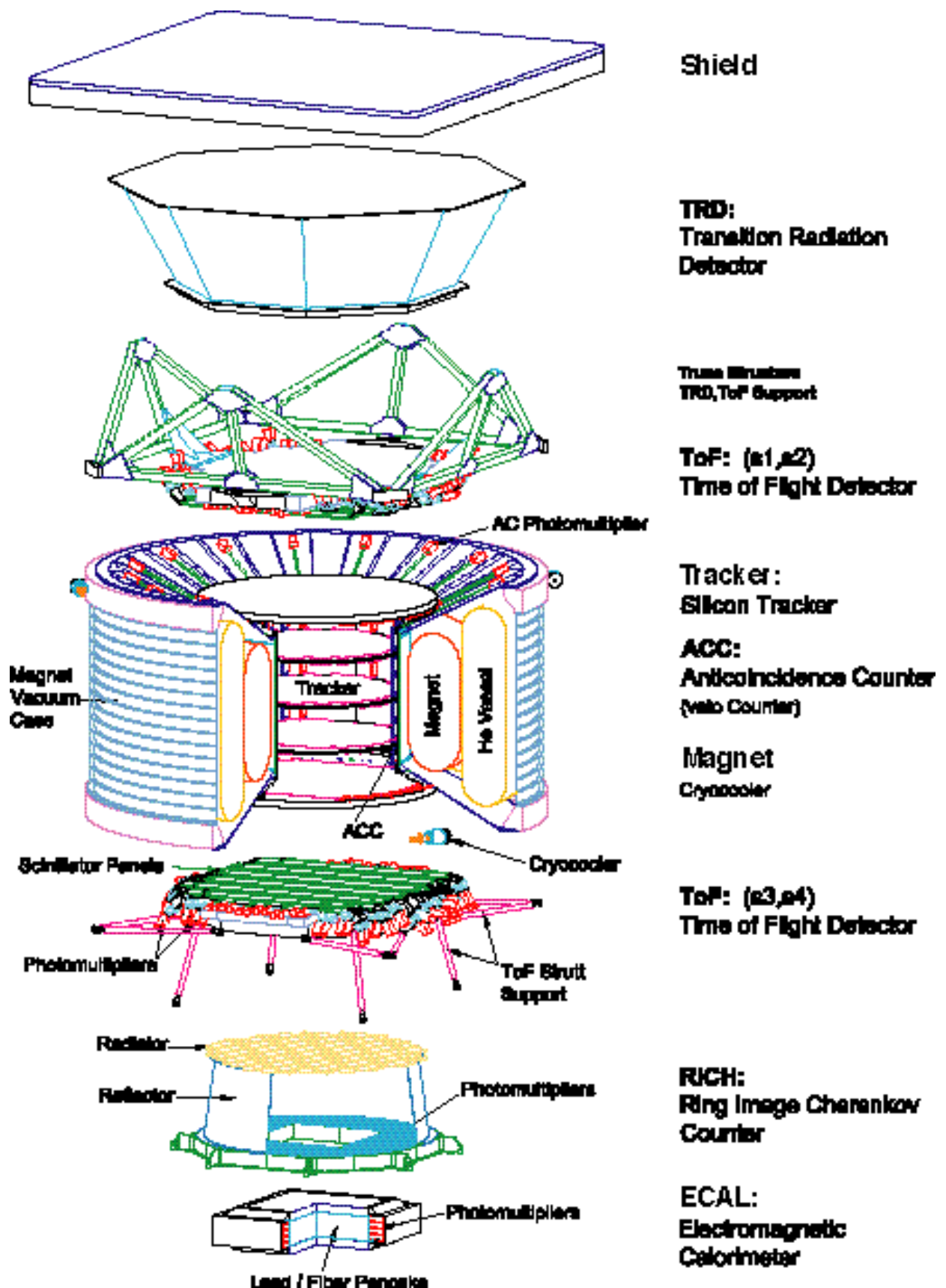


Figure 41 : Schematic of the Detector Assembly on the Magnet.

II. Transition Radiation Detector (TRD)

1) Introduction

The AMS-02 TRD detector is located on top of the magnet vacuum case as shown in Figure 42 (as well as Figures 4 and 26). A charged particle traversing this detector produces characteristic electromagnetic radiation depending on its mass and momentum. Since the particle momentum is determined by the silicon tracker with excellent accuracy, the detected transition radiation (TR) is used to distinguish between particles of different masses. The design and construction of the TRD system is a collaborative effort of RWTH Aachen and MIT under the leadership of K. Lübelmeyer, S. Schael and U.J. Becker, supported by P. Fisher, J. Burger, K. Scholberg and others.

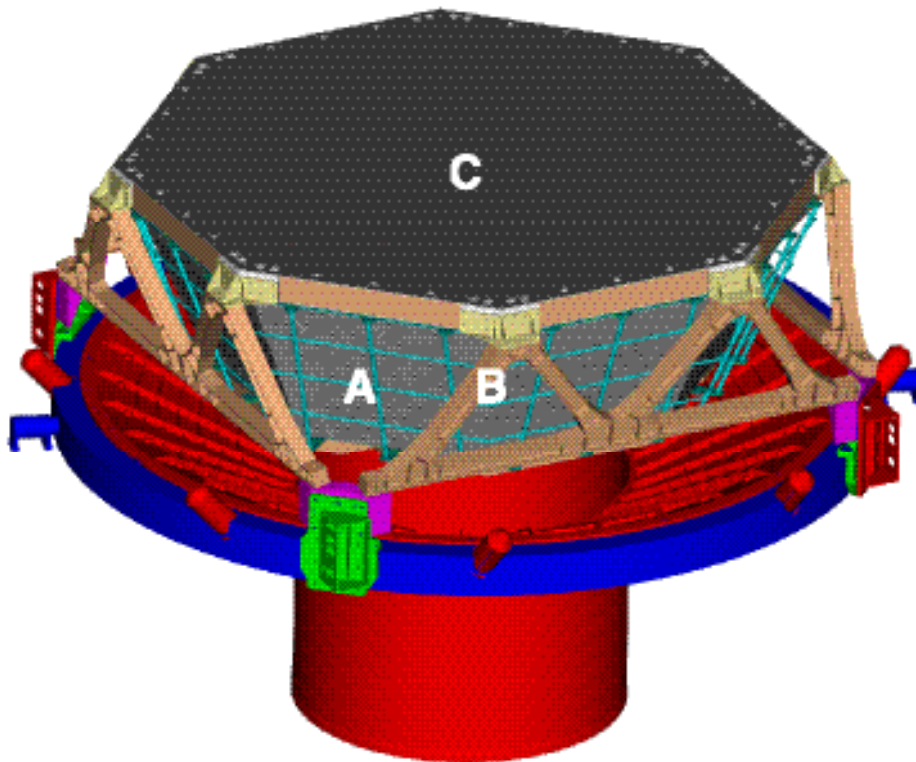


Figure 42 : Computer aided view of the AMS-02 TRD on top of the magnet vacuum case.
(A) TRD body with octagon side walls. (B) Support Structure (M-structure).
(C) Top Honeycomb.

Transition radiation is the electromagnetic radiation emitted when charged particles traverse the boundary between two media with different dielectric properties ϵ_1 and ϵ_2 . It is the result of the modification of the particle's field when traveling from a medium with ϵ_1 to a medium with ϵ_2 . The probability for a particle to emit a TR photon at a single interface is small (10^{-2}). This can be significantly enhanced by a multilayer structure, for example by a 20 mm thick

fleece as radiator. The TR photons are detected in straw tubes, filled with a Xe/CO₂ (80%/20%) gas mixture (see Figure 43) and operated at 1600 V. The detection probability of TR photons is about 50%.

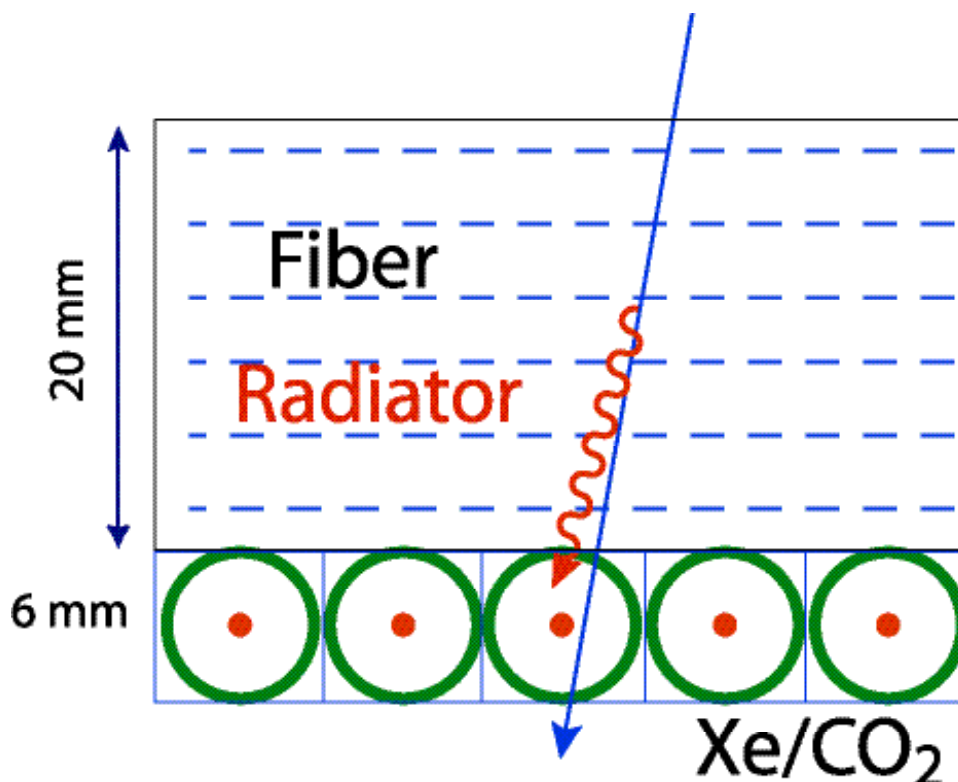


Figure 43 : Working principle of the AMS-02TRD.

The principle of TRD's is very well understood and they are used in large particle physics experiments like ATLAS and HERA-B. The challenge is to operate such a large gas detector safely and reliably in space for 3-5 years.

2) Mechanical Structure

The TRD consists of 20 layers of straw modules interleaved with a fiber fleece material and arranged in a conical octagon structure as shown in Figure 44. Each straw module contains 16 tubes arranged side by side. The top and the bottom 4 layers of straws are oriented parallel to the main component of the magnetic field while the middle 12 layers are orthogonal. The length of the straw modules varies from bottom to top layer from 0.8 m to 2.0 m. The total number of modules is 328 for a total of 5248 wires. On the outside of the conical octagon structure a grid structure (see Figures 42 and 44), built out of carbon fiber tubes, is attached to support the services (gas tubes, HV cables, signal cables).

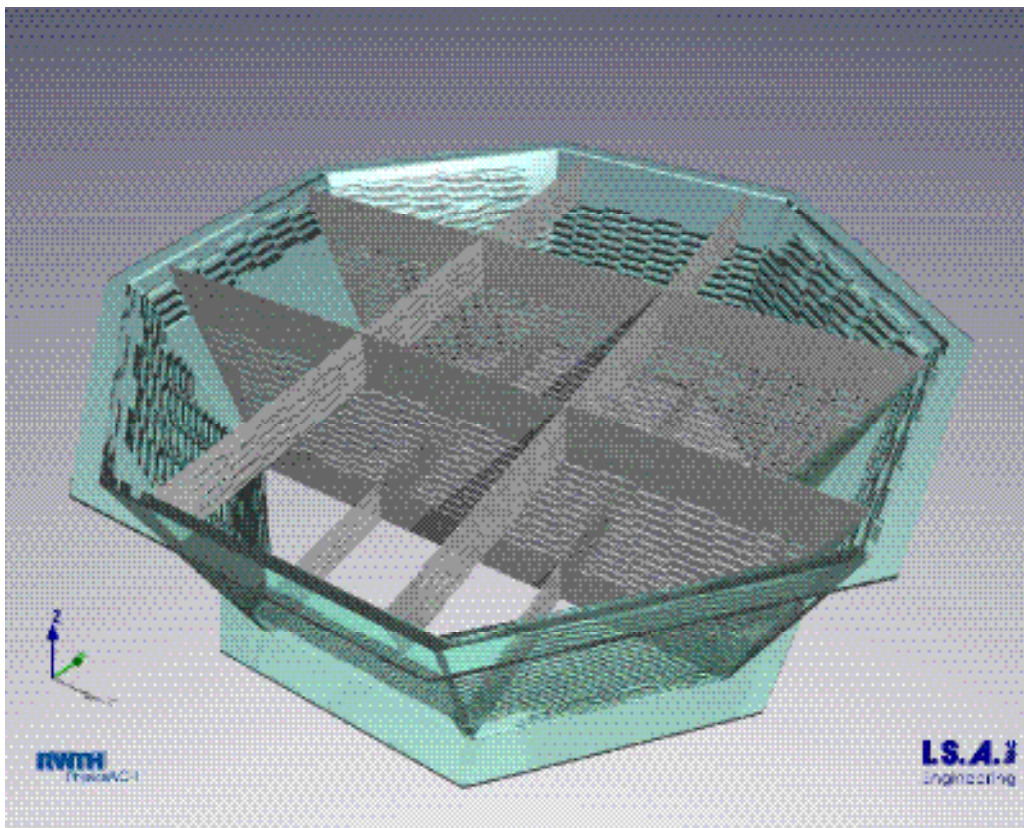


Figure 44: Computer generated view of the TRD support structure.

One 16 straw tube module is shown in Figure 45. The straws have an inner diameter of 6 mm, the wall material is a several layer aluminum-kapton foil with a total thickness of 72 μm . A gold plated 30 μm thick tungsten wire, fixed in a polycarbonate end piece, is used as sense wire. The crimping technique used for the connection between the tungsten wire and a CuTe-end piece has been developed in Aachen. It has been used for the production of the L3 hadron calorimeter endcap chambers and the L3 forward-backward muon chambers which have been operated successfully during the last 10 years at the LEP collider at CERN. The straw modules are mechanically stabilized by longitudinal and vertical carbon fiber stiffeners.



Figure 45: TRD straw module as produced for the CERN 2001 testbeam.

For the operation of the TRD detector in space the gas tightness of the straw modules is a key point. Detailed tests have shown (see Figure 46) that the gas tightness of the end pieces is excellent and the leak rate for one straw of 0.3×10^{-6} l mbar/s/m is dominated by the diffusion through the straw walls. Assuming pure diffusion leaks this would correspond for the data taking period of 1000 days on the ISS to a loss of 50 liters Xe and 170 liters CO₂ gas equivalent to a total leak rate of 10^{-5} mbar/s.

Allowing for gas leaks (different from diffusion) of 10^{-4} mbar/s the required gas storage (80% Xe, 20% CO₂) amounts to 1760 liters Xe and 440 liters CO₂ gas. We will carry 50 kg of gas corresponding to 8100 liters Xe and 2000 liters CO₂ at 1 atm, resulting in a safety factor of ~ 5. It can also be used for refreshing the circulating gas.

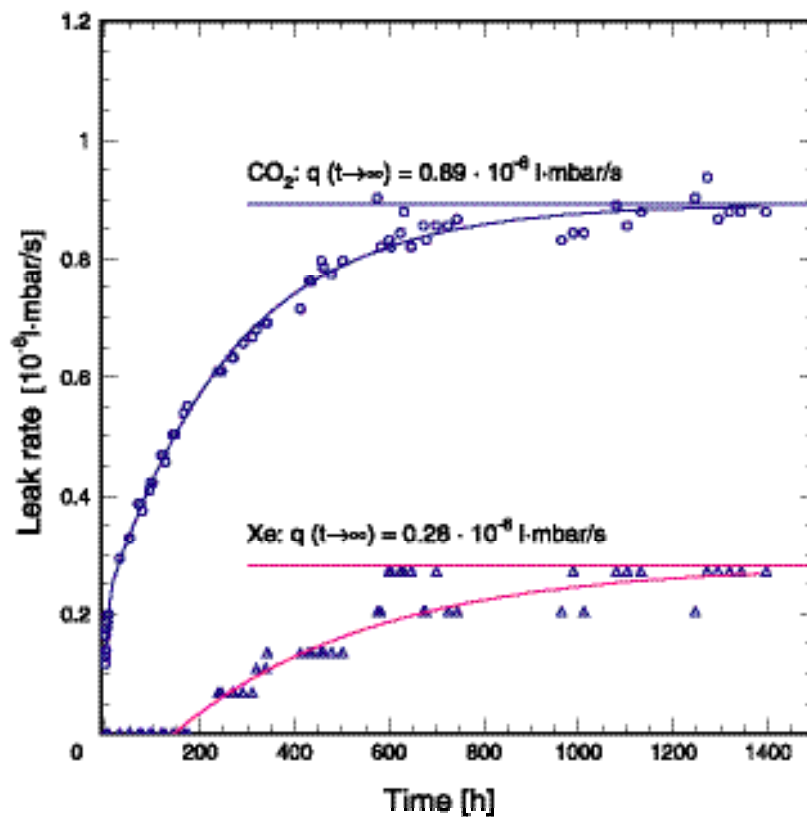


Figure 46: Gas leak rate as measured with a mass spectrometer for Xe/CO₂ (80%/20%) with three 1.3 m long straws connected in series

The octagon structure is built out of a carbon fiber and aluminum honeycomb sandwich material. The structure is machined with a precision of 100 μm, corresponding to three sense wire diameters. For the sidewall an aluminium honeycomb 26 mm thick and 2 layers of 2 mm thick Carbon Fiber Composite (CFC) material is used. The octagon structure is closed by two plates. The lower one has a total thickness of 41 mm (2 × 0.5 mm CFC and 40 mm aluminium

honeycomb) and the upper one 94 mm (2 × 1.0 mm CFC and 92 mm aluminium honeycomb). A reinforcement ring is added on the upper plate for mechanical stability. The upper plate is supported by an aluminum M-structure which is attached to the Unique Support Structure (USS) which is built by NASA as an interface between AMS and ISS (see Figure 26). The M-structure will be closed by 10 mm thick aluminium honeycomb sandwich plates (2 × 0.5 mm Al-sheets, 9 mm aluminium honeycomb) which act as debris shielding and also enhance the inplane stiffness of the M-structure.

3) Radiator

Standard radiators for transition radiation detectors are made of 15-20 µm thick polypropylene foils with a regular 200-300 µm spacing between them. Such radiators provide the highest transition radiation yield, but the specific detector geometry and space qualification do not allow the use of a regular foil radiator.

Recent studies by the ATLAS collaboration have shown that a radiator made of polyethylene/polypropylene fibers performs nearly as well as a regular foil radiator when the fibers are oriented obliquely to the particle direction. This kind of radiator is used in the AMS-02 TRD.

The manufacturer of the fleece material LRP 375 BK is at Freudenberg Vliesstoffe KG, Germany. The fiber thickness is 10 µm and the fiber sheets have a density of 0.06 g/cm³ and a thickness of 5 mm. Each straw module will be covered by 20 mm of this fleece material for a total amount of 210 m² for the entire TRD.

A crucial point is the space qualification of the materials used in the detector. The deposition rate on nearby attached payloads on the ISS is 10⁻¹⁴ g/s/cm² corresponding to a maximum allowable outgassed mass flow rate of the radiator material of 10⁻¹² g/s/cm². A measurement of the outgasing rates with respect to the NASA-ASTM E 1595 report has shown that this limit of 10⁻¹² g/s/cm² was reached after cleaning the fleece material with CH₂Cl₂ (so-called 'soxhlet' extraction method). At the CERN beam test of the summer 2000 (Figure 47), we show that the cleaning of the fleece does not affect the transition radiation performance .

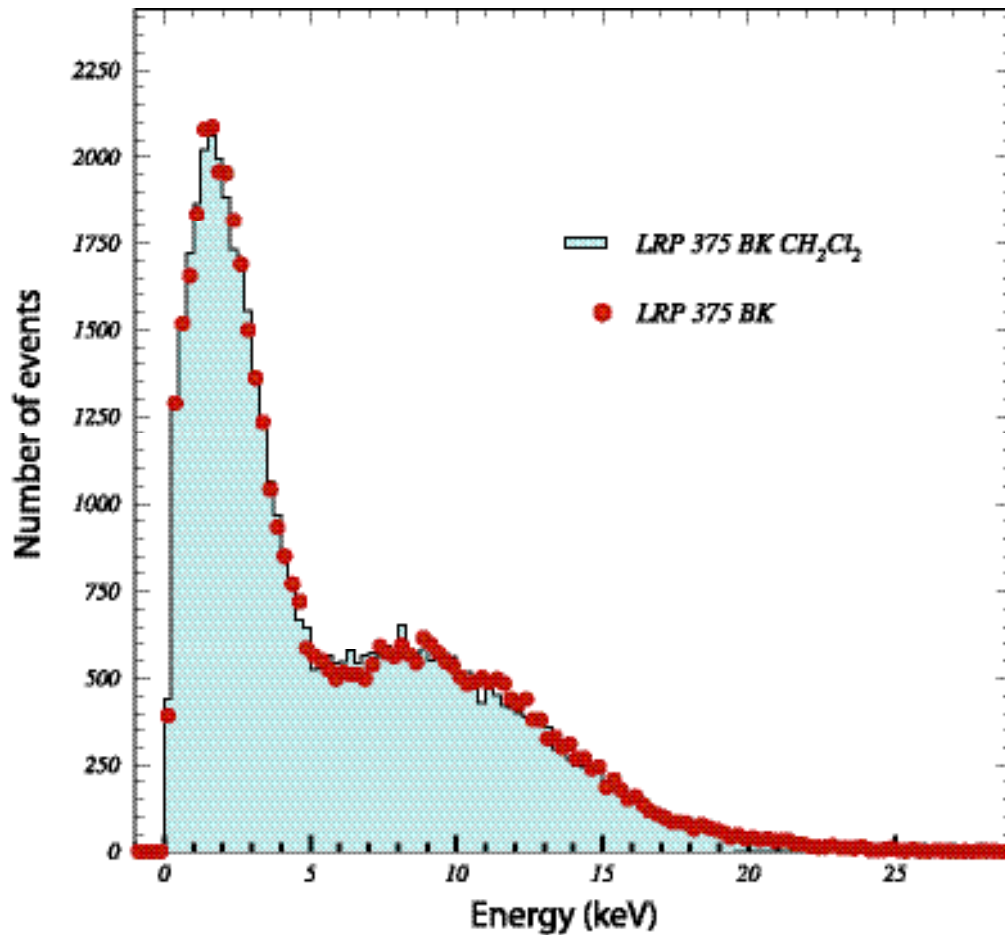


Figure 47: Single straw spectrum with LRP 375 BK fleece material in front of the straw modules in comparison to a spectrum with LRP 375 BK cleaned with CH_2Cl_2 .

The fleece material has already been produced and cut in 100 mm wide bands by Freudenberg Vliesstoffe KG. The various pieces will be cut to the appropriate length in Aachen and will then be cleaned by the Institute of Organic Chemistry of the RWTH Aachen by September 2001.

4) Front End Electronics and DAQ System

The DAQ system of the TRD is divided into two parts as shown in Figure 48 : the front-end electronics which is mounted on the octagon walls of the TRD, and the first level of data acquisition which is hosted in two identical crates next to the TRD.

The digitization of the signals from the 5248 straw tubes is done in the front-end electronics. It consists of the following :

- UTE board
Each detector module is equipped on one end with a printed circuit board called UTE. On the 'module side' the 16 wires of the straw tubes are soldered, on the 'electronics side' connections for the HV input and the 16 signal outputs are implemented. The purpose of the UTE board is to distribute the high voltage to all 16 wires of each module and to decouple the high voltage from the wire signals.
- UHVD board
Each group of four detector modules is biased from one channel of the high voltage unit which is located in the DAQ crate. One UHVD board and a coaxial cable are used to feed the high voltage to all detector modules of one group.
- UFE board
One group of four detector modules is connected to one readout board called UFE, performing amplification, shaping and digitalization of the signals of each wire of the four modules.

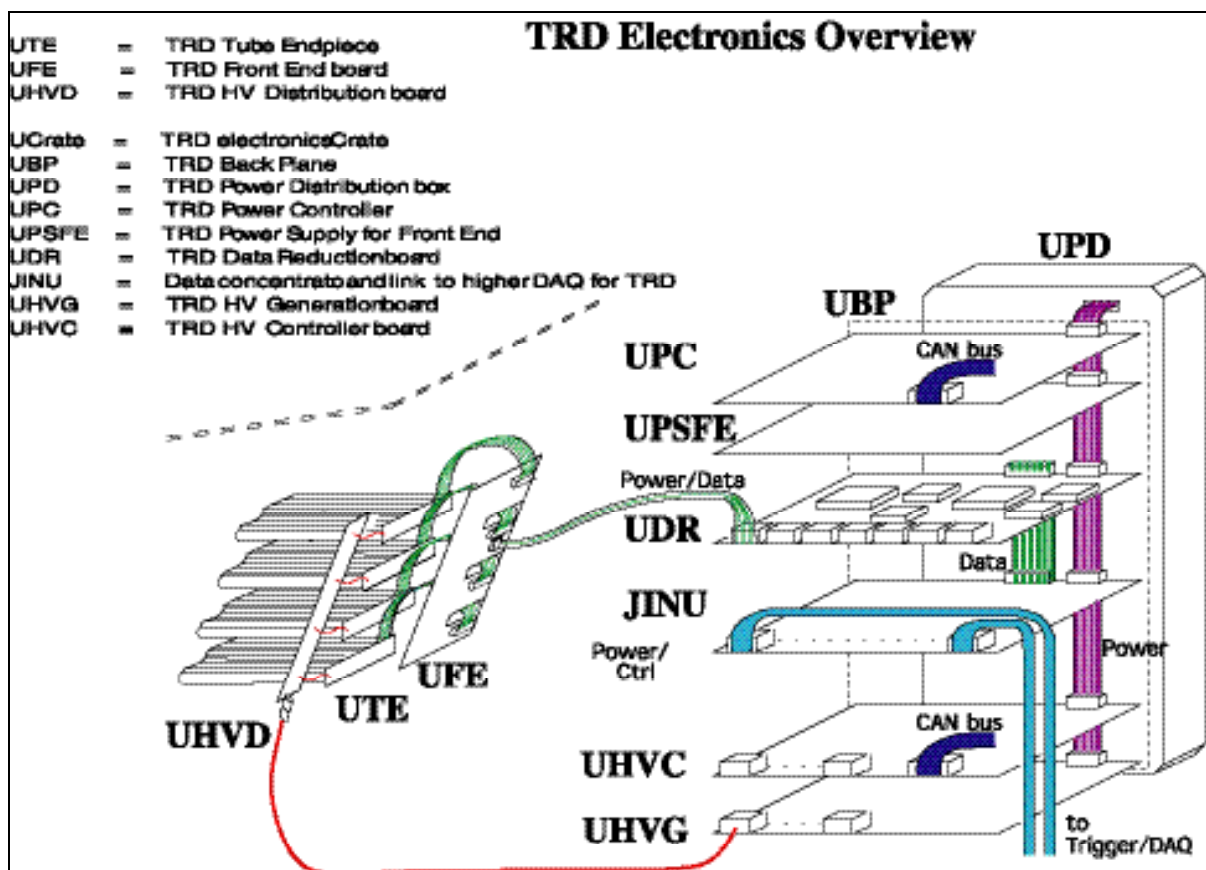


Figure 48 : Schematic view of the TRD electronics.

The crate hosts the power supplies, the boards which collect and compress the data and the control of the TRD DAQ system. The electronic crates consist of the following modules:

- The **UPD** (Power Distribution box) contains the DC/DC converters for the various boards. Each DC/DC converter is doubled for redundancy.
- All voltages are distributed to the different boards via the backplane **UBP**. Also all control and data lines for inter-board communication are implemented in the **UBP**.
- The **UPC** monitors and controls the power of all boards in the TRD crate. Each DC/DC converter and electronic board in the crate can be switched on and off separately. The **UPC** is also used for the readout of the temperature sensors.
- The **UPSFE** board regulates and distributes the voltage for the front end electronics. Each UFE board has its own power line and control for digital and analog parts.
- The **UDR** board reads the digitized data from 7 UFE boards. The front end voltages (± 2.0 V), which are generated in the **UPSFE**, are piped through the **UDR** so that only one cable with 18 twisted pair lines is necessary to connect an UFE board with the crate electronics. The **UDR** board receives the level-1 trigger, generates the read out sequence for the UFE boards and reads the data from the 7 ADCs in parallel. A Digital Signal Processor (DSP) compresses the data (mostly pedestal subtraction), attaches the appropriate geographic address and on request sends the data to the **JINU** board. For redundancy the **UDR** has two complete digital units, of which only one is switched on at a time.
- The **JINU** board collects the data of all **UDR** boards and transfers them to the higher DAQ system of AMS-02.
- The **UHVC** board controls and monitors the HV generated on the **UHVG** board via CAN bus.
- On the **UHVG** board a Cockcroft-Walton elevator multiplies the input voltage of +120 V to max. +2000 V. The HV is controlled via a special chip which communicates with the **UHVC**.

5) Module Production and Quality Control

After the successful production of 60 TRD modules for the test beam measurements in summer 2000 (see section VII) the following procedures for quality insurance and quality control have been established.

(i) Step One :

The individual straws are cut to length and glued together with the longitudinal and transversal stiffeners on a precision jig (see Figure 49) developed in Aachen. This operation takes place in a clean room installed at the company FVT in Aachen.

Then the straw modules are transported to the workshop of the First Physics Institute of the RWTH Aachen. Here the polycarbonate endpieces are glued to the straw modules. This is also done in a clean area with controlled environment.



Figure 49: Precision jig for the straw module assembly.

(ii) Step Two :

The second step is the wiring, tensioning and crimping. A signal feedthrough measurement is applied to all wires, so that broken wires can be found and replaced. The wire tension 100 ± 10 g is controlled for each wire via an eigenfrequency measurement. The noise level of each wire is measured by counting the discharges over a time period of 100 s. For this high voltage is applied to the straw module which is placed in an Ar/CO₂-atmosphere. Finally all wires are checked again with a signal feedthrough test.

(iii) Step Three :

The third step is the high-voltage board mounting and the final potting of the straw module endpieces.

The produced straw modules undergo the following operational tests:

(i) Serial test :

- Overpressure burst test: The gas tightness of each straw module is checked up to an overpressure of 2.5 bar.
- Pressure drop test: The Ar/CO₂-leak rate of each straw module is measured by a pressure drop test at 2 bar in a vacuum vessel. A straw module is gastight when the measured leak rate is less than 10^{-4} mbar/s.
- Dark currents: The operational high-voltage range of (1500-1600) V corresponds to a straw gas gain in the range of (2-5) 10^3 in a Xe/CO₂ (80%/20%) gas mixture . The straws should operate without any significant (< 1 nA) dark current over this high-voltage range.

(ii) Gas gain measurement:

The calibration of each straw is done by measurement of the gas gain as a function of the high voltage. The straw-signals are caused by converted 5.9 keV photons emitted by an Fe⁵⁵ source.

(iii) Long term test :

The aim of the long term test is to study the long term behavior of the straw modules. Eight (16 tube) modules are mounted in a vacuum vessel. This is the equivalent of a TRD gas circuit. The Xe/CO₂ gas mixture is flushed through the 8 chambers in series at 1.0 l per hour in a closed circulating gas system. The gas gain is measured using the signals of converted 5.9 keV photons of an Fe⁵⁵ source.

(iv) Wire displacement :

For samples of the straw modules the wire positions with respect to the straw walls are measured using an X-ray photograph.

The mass production of TRD modules should be finished by summer 2002.

6) Space Qualification

(i) Structural Verification

- Analytical Method

A coupled load analysis of the entire TRD structure based on the "structural Verification Plan" (NASA JSC-28792, Rev. A) has been carried out by means of a detailed Finite Element Calculation (F.E.C.). The first natural eigenfrequency turns out to be 67.1 Hz, well above the required 50 Hz. Figure 50 shows for the most critical direction, the z-direction, the relative deformations.

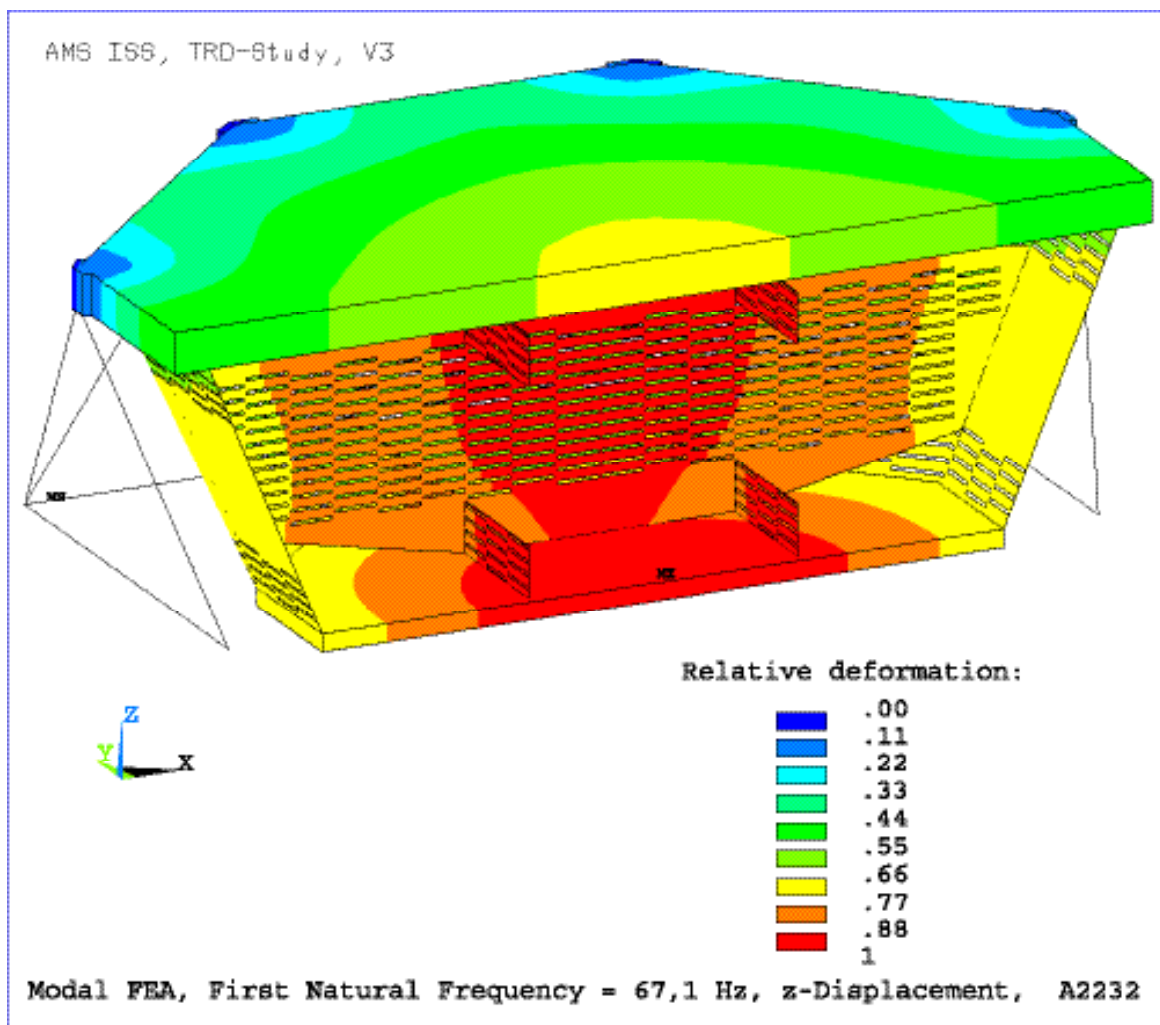


Figure 50: TRD modal analysis results. The relative amplitudes of the deformations of the TRD structure in the Z direction are shown for its lowest natural eigenfrequency. It is 67.1 Hz.

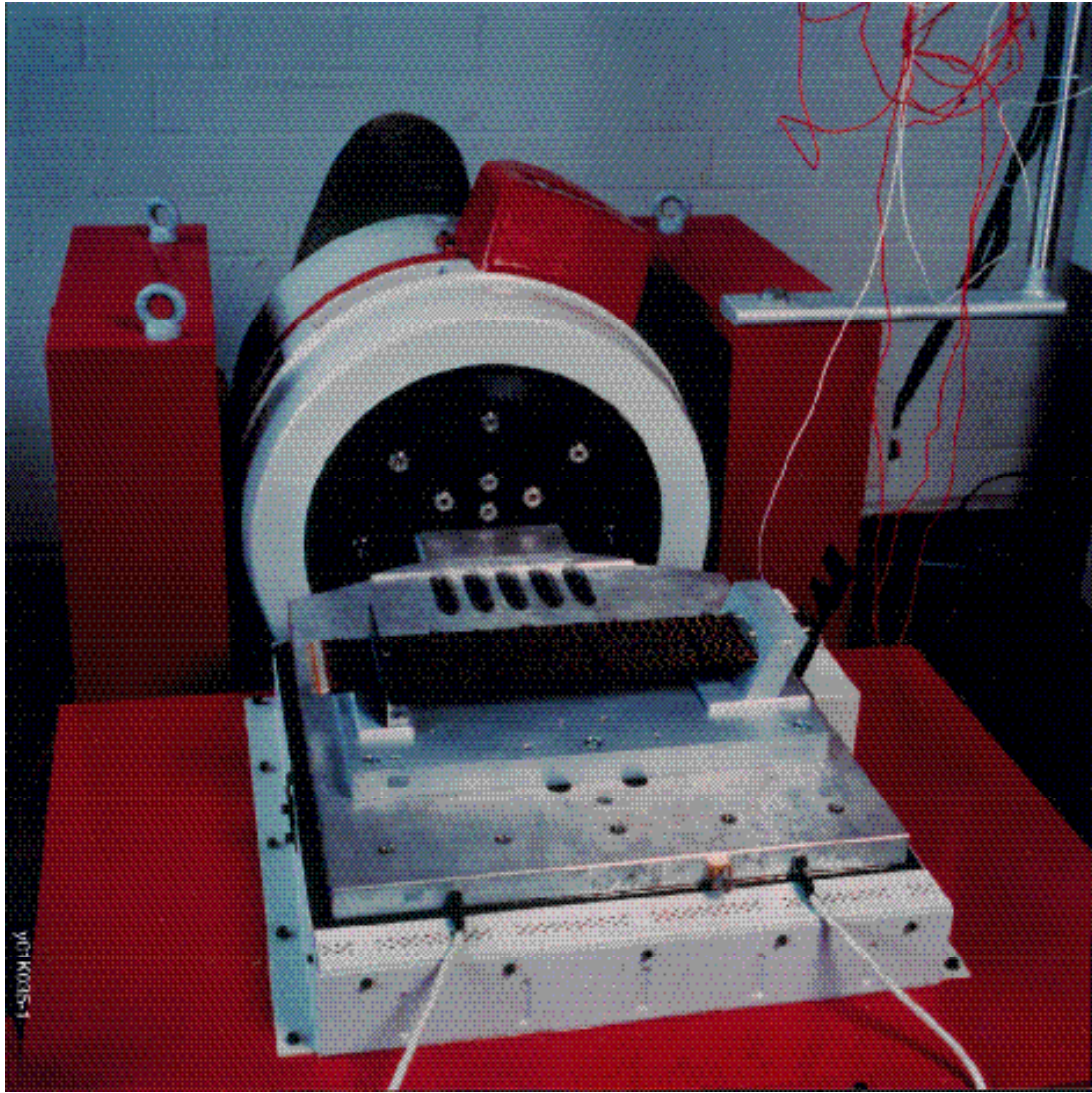


Figure 51 : Vibration test stand loaded with a TRD straw module at the RWTH Aachen.

- Experimental Verification

Experimental tests are carried out (see Figure 51) to verify material properties and analytical calculations :

a) Straw modules

Four 1.4 m long straw modules undergo the following tests :

- Vibration Test
This is a 0.5 g sine sweep followed by a 6.8 grms random vibration test followed by a 0.5 g sine sweep.
- Acoustic Test
This is a test of the four modules with a sound pressure level of 115 db.
- Thermo Vacuum Test
This is an 8 cycle thermo vacuum test between -20°C and $+40^{\circ}\text{C}$ of the four modules.

- EMI Test (Electro Magnetic Interference)
An EMI test of the four modules were carried out.

b) Octagon Panels and CFC Honeycomb Plates

- Separate static load tests (according to the NASA Structural Verification Plan) on the face sheets and the final honeycomb-face sheet composite structure are carried out on material samples.
- Static load tests on the various kinds of inserts are performed.
- Samples undergo thermo vacuum tests in a temperature range from -20°C to $+40^{\circ}\text{C}$.

c) M. Structure and Brackets

- Static load tests are performed.

(ii) Electronics

The qualification boards of the electronic components will undergo the following tests :

- Vibrations Test
 - Thermo Vacuum Test: 8 cycles from -20°C to $+60^{\circ}\text{C}$.

(iii) TRD Gas Tubes

The TRD gas tubes operate during ground operation and lift-off/landing with a Xe/CO₂ gas pressure of 1 atm inside and 1 atm outside. On orbit they will operate with the same inside pressure but now against vacuum.

- Overpressure test – to 2 atm overpressure for a safety factor of 2.

(iv) Material Properties

All materials are space-qualified according to NASA regulations.

7) Test Beam Results

To verify the performance of the proposed TRD design a 20 layer prototype detector was built from 2×20 modules, each 400 mm in length and covered with 20 mm of fleec radiator in front. The Xe/CO₂ (80%/20%) mixture was flushed through the chambers at 0.3 l per hour in six open-ended gas-circuits each connecting 6 or 8 modules in series.

During three beam test periods in summer 2000 at CERN, 3 million events were recorded providing signal responses for protons, electrons, muons and pions at energies between 5 GeV and 250 GeV. Muon events were used to intercalibrate the individual straws to a relative accuracy better than 2%. For the absolute energy calibration an Fe^{55} source emitting 5.9 keV photons was used. The environmental influences on the gas gain, temperature and pressure were monitored continuously. To determine the electron-efficiency and proton-rejection a sample of clean single track events was preselected. For these events Figure 52 shows the energy depositions in each straw for 20 GeV protons and electrons. The detection of TR photons is clearly visible in the electron-spectrum at energies above 5 keV.

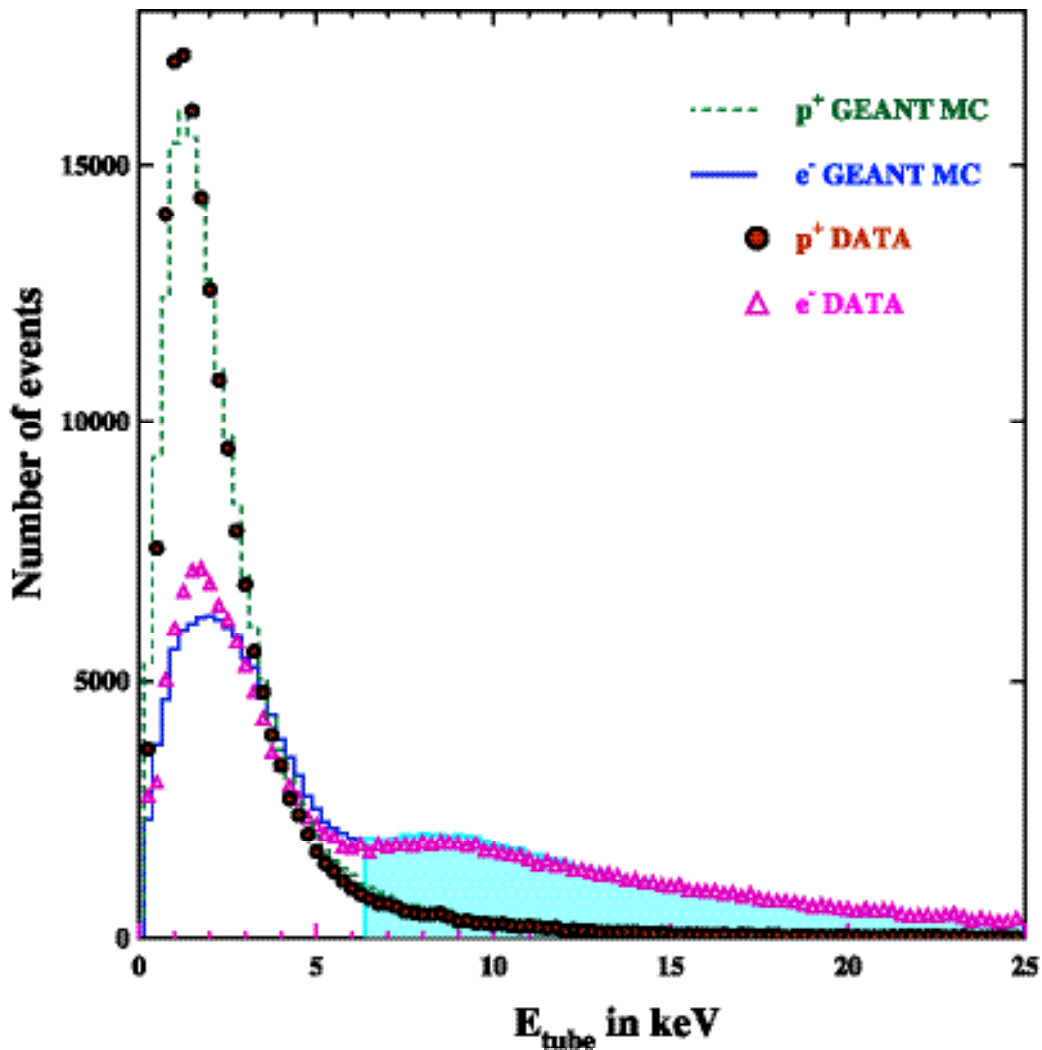


Figure 52: Single straw energy deposition spectra for 20 GeV protons and electrons, normalized to the same number of entries. The plot contains all hits on a track with the colored area marking the hits above 6.5 keV interpreted as TR-clusters.

Particles are then identified based on a simple cluster counting algorithm. In at least 6 layers out of 20 a straw close to the track with an energy deposit above 6.5 keV was required. This selects electrons with 90 % efficiency and rejects over 99% of the protons up to 200 GeV as shown in Figure 53. In other words, over the full energy range the required proton rejection power of 10^{+2} is more than fulfilled. The proton rejection is an upper limit since inclusion of corrections due to beam impurities, which are still under investigation, will improve the result. Further improvements are expected from using more sophisticated analysis tools like maximum likelihood methods or a neural network.

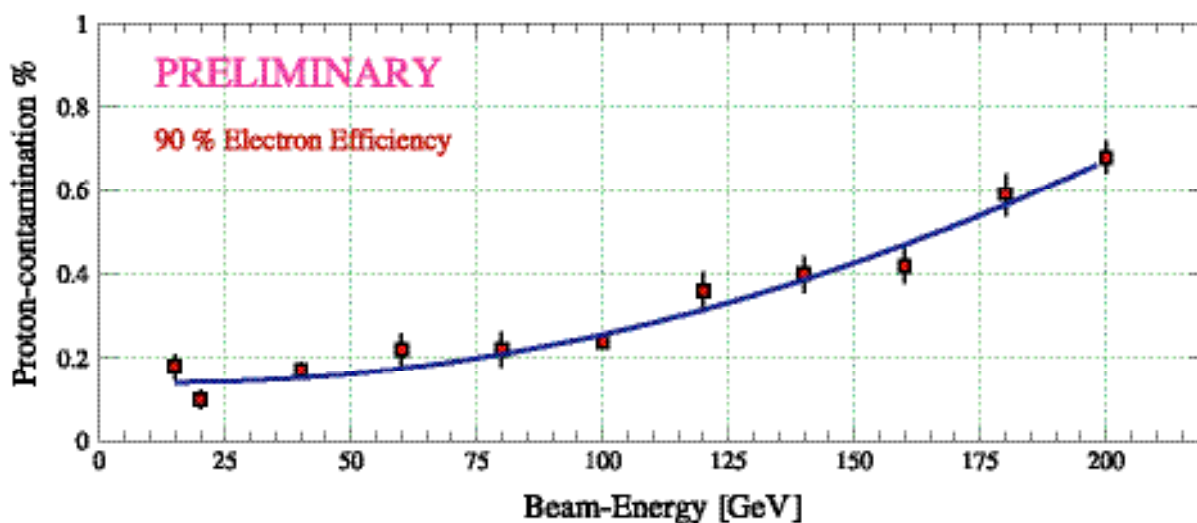


Figure 53 : Proton contamination in the electrons for 90% electron efficiency from clean single track events with a cluster counting algorithm. These numbers are upper limits as they are not yet corrected for the pion contamination of the beam.

8) TRD Simulation

K. Scholberg (MIT) is coordinating the TRD subdetector simulation in the main AMS Monte Carlo (developed by V. Choutko and A. Klimentov). The transition radiation simulation is based on tables provided by V. Saveliev of DESY; the TR simulation matches well the beam test data taken at CERN in 2000 for electrons up to 100 GeV. The dE/dx simulation in thin gas layers is currently also being tuned to match the beam test data, in collaboration with RWTH-Aachen.

Preliminary studies using the full AMS Monte Carlo indicate proton rejection at the 10^{-3} level.

9) Thermal Model

The thermal stability of the TRD is essential for the performance of the detector during its operation on the ISS. Temperature variations change the gas density and hence the gas gain.

To keep these uncertainties at a few percent level, comparable to the module to module inter-calibration uncertainties, temperature gradients within the TRD should not reach a level of more than ± 1 K. A first thermal control study has been performed by OHB System, Bremen, Germany. The results are summarized as follows.

In order to prevent low temperatures the experiment must be covered almost completely by MLI, (Multi Layer Insulation) except a small "thermal window", which serves as heat sink and radiates the TRD dissipation (20 Watt, UFE boards) to the environment. The thermal radiator area is foreseen adjacent to the upper TRD cover. These surfaces will radiate only into the Zenith direction. The shape of the thermal radiator is a symmetric extension of the upper TRD cover in order to have a continuous radiator area at the circumference of the TRD.

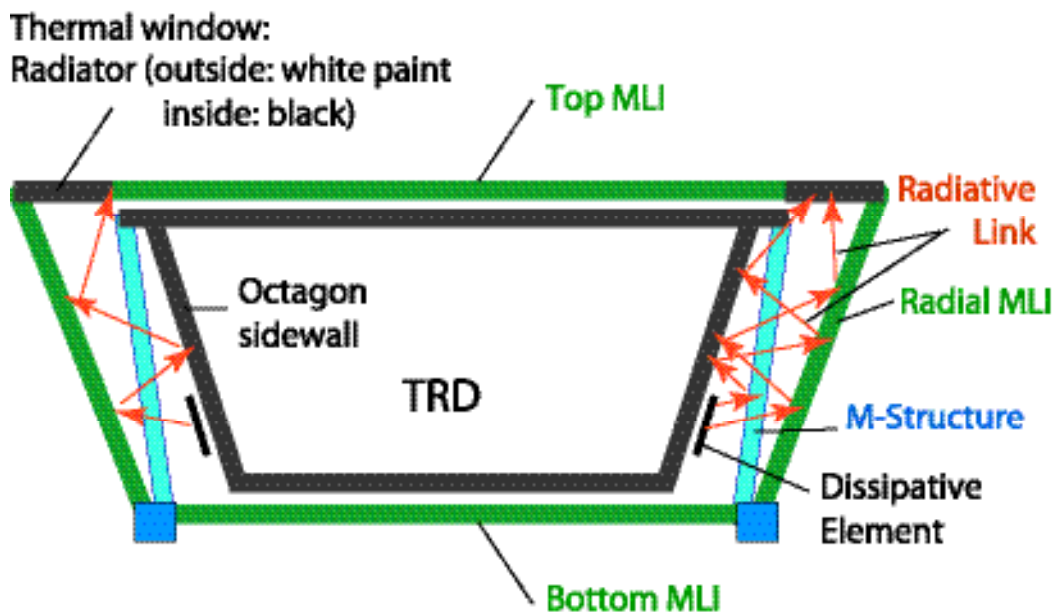


Figure 54 : Schematic of the radiative link to the radiator.

It is foreseen to couple the dissipative elements (UFE boards) to the thermal radiator by radiation as shown in Figure 54 (red arrows). A thermal analysis shows that the needed radiator surface is only 0.061 m^2 . The uniform temperature on the octagon side walls will prevent temperature gradients also across the octagon (Kapton/Fleece compound).

The dissipative elements (UFE boards) with a high emissivity surface on the outside and low emissivity on the backside will radiate heat into the cavity formed by the octagon side walls, radial MLI and radiator bottom side. The infrared emission will be reflected by the high reflective MLI foil and partly absorbed by the octagon side walls and radiator bottom side. Also

the octagon side walls will emit infrared radiation, which is reflected at the MLI foil and absorbed by the radiator. The M-Structure trusses will be painted black which increases the thermal mass considerably (see Figure 42).

The relevant results of the thermal analysis are shown in Figure 55 and 56. These studies indicate that it is realistic to fulfill the requirement of a maximum temperature gradient within the TRD structure of ± 1 K. A contract with OHB System has been placed for detailed thermal studies of the TRD. The results of this study will be integrated by Carlo Gavazzi Space (Milan) into the overall AMS-02 thermal model.

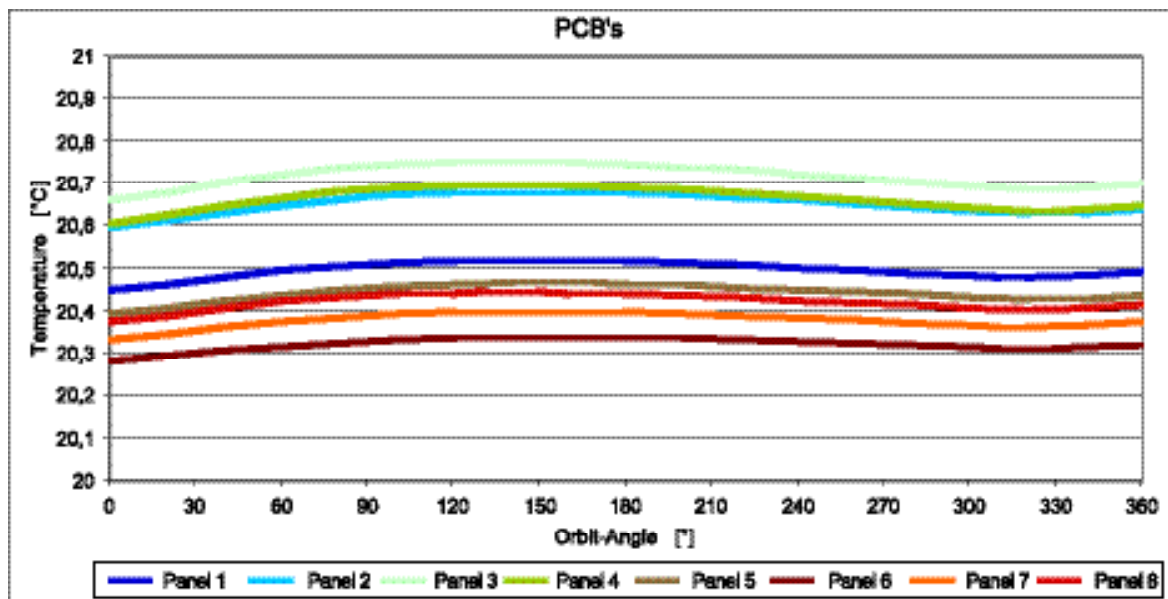


Figure 55: Analysis results for the PCB (UFE boards) temperature. The calculation is done for points on the eight octagon sidewalls (panel 1 through panel 8) for a typical orbit.

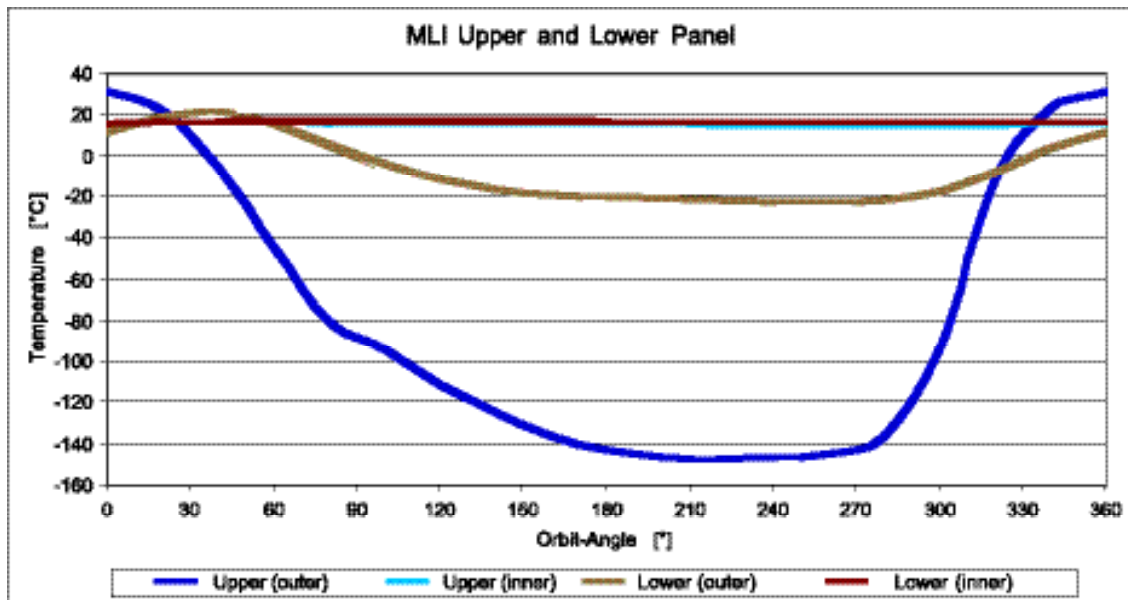


Figure 56 : Analysis results for the upper and lower MLI temperature. The calculation shows that the temperature variation on the outer surfaces of the Top (upper) and Bottom (lower) MLI are not transmitted to the inner surfaces of the MLI nor to the TRD structure.

10) The AMS-02 TRD Gas System

The MIT Group of U. Becker, J. Burger et al. has many years of successful experience in studying gas detector systems, including the original development of high rate multiwire chambers for the BNL J experiment, the development of drift tubes for the Mark J detector, and the construction of the 1000 m³ L3 muon system which had a resolution of 30 μ and operated over 10 years without failure. The TRD gas system, which is the critical part of AMS, is the responsibility of U. Becker, J. Burger, P. Fisher et al. A schematic view of the TRD Gas System is shown in Figure 57. The TRD will use a mixture of Xe/CO₂. During TRD operation the Xe/CO₂ 80/20 gas is circulated through the TRD detector by pumps in Box C several times per day. The performance is monitored by calibration tubes in Box C. Box S provides 7 liters of fresh gas daily to the TRD.

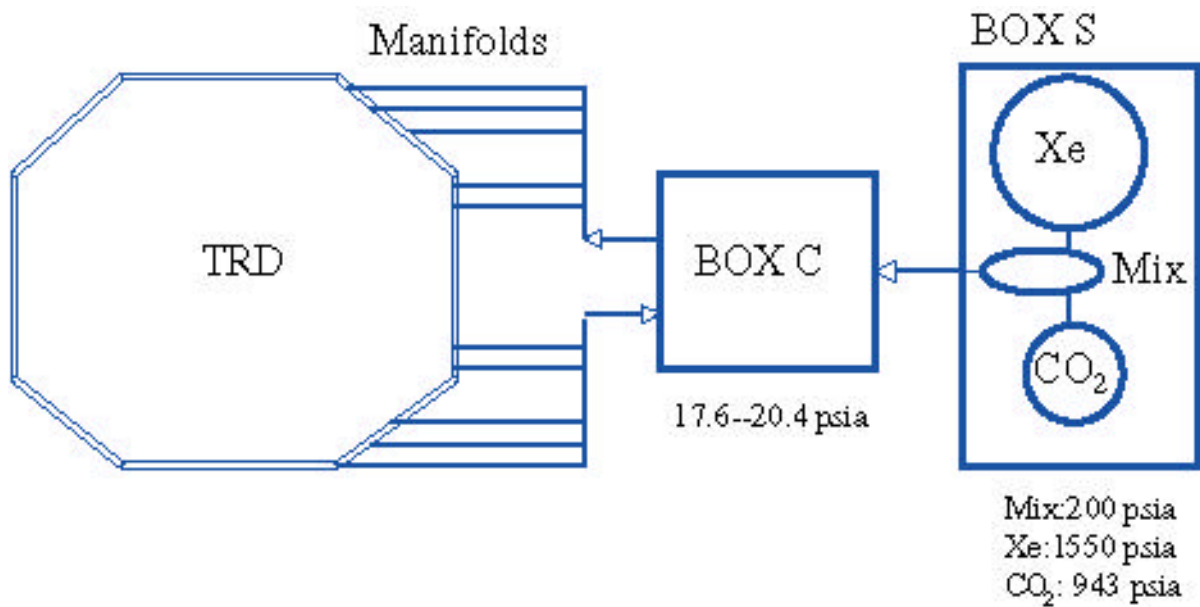


Figure 57 : Overview of the TRD Gas System. Pressures at 25°C.

(i) **Box S**

The flow diagram for the supply box (Box S) is given in Figure 58. It transfers a controlled amount of gas from the Xe and CO₂ containers into the daily buffer vessel D.

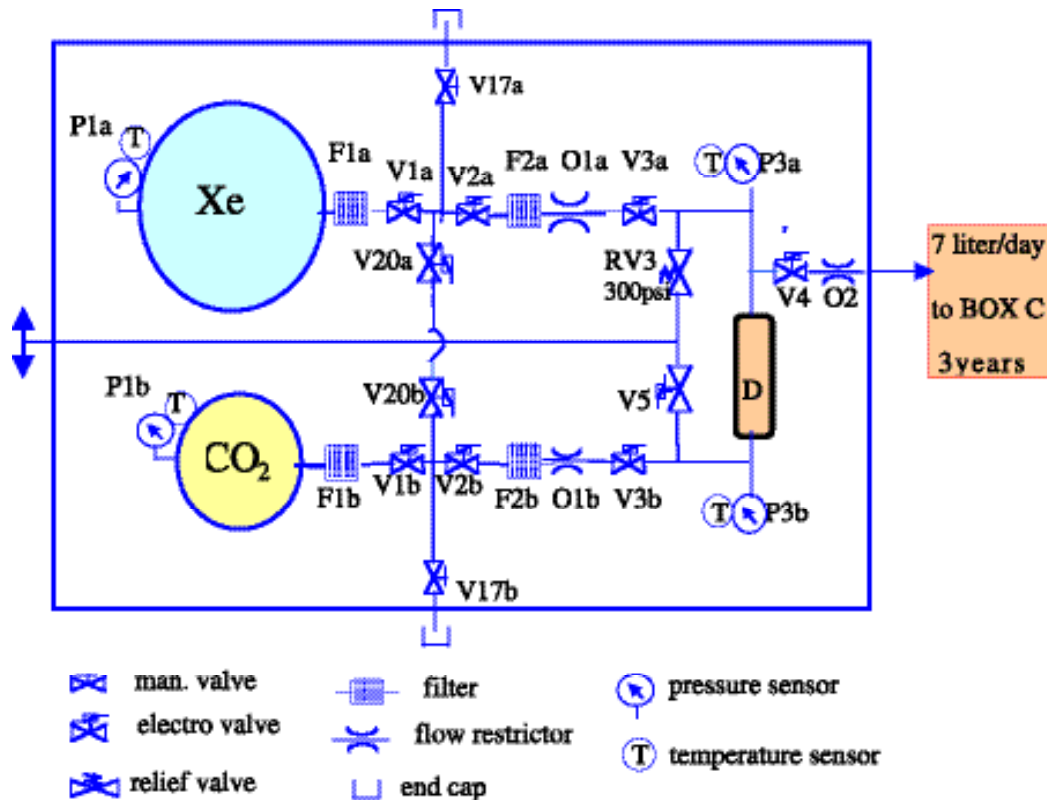


Figure 58 : Schematic for Box S.

The gas from the supply vessels, marked Xe and CO₂, is filtered (F1a, F1b, F2a, F2b) and then metered into known quantities trapped in the tubing between solenoid valves (V1a, V2a, V1b, V2b). Subsequently the flow is controlled via flow restrictors (O1a, O1b). Gas from the two supply vessels is added to vessel D by using V3a and V3b; the mixture is controlled by measuring partial pressures with P3a or P3b. Relief valve RV3 insures that NASA safety regulations are met and that no part of the system is exposed to excessive pressure. Three valves in series (V1a, V2a, V3a or V1b, V2b, V3b) and a flow restrictor (O1a or O1b) protect the rest of the TRD gas system from the high pressures of the supply vessels.

We are working together with Arde Inc, who have extensive experience with the Space Station and the Shuttle projects, for the manufacture of the pressure vessels (Xe: ARDE D4636, CO₂: ARDE D4683, D Mixing Vessel: ARDE SDK 13181) and the construction of the flight version of Box S.

Special cleaning procedures are used for the Marotta MV100 high pressure valves (V1a, V2a, V3a, V1b, V2b, V3b) and other pipes and fittings. The MV100 valves have been tested and found to be leak tight up to 8000 Gauss. This exceeds the fringe fields of 300--1500 Gauss at the location of Box S. Studies on the mass flow as a function of time with the valve opened have been performed succesfully. Future studies will include the effect of magnetic fields on valve endurance. A study of the effect of CO₂ freezing in the valve when it adiabatically expands is planned. Prototype driver circuitry for the valves has been built and tested. The INFN-Rome group will perform the flight design under the leadership of B. Borgia and S. Gentile.

Lee Viscojet flow restrictors (O1a, O1b) utilizing special geometries with openings 10 times larger than regular flow restrictors, hence reducing clogging problems, have been acquired. These restrictors require the same cleanliness procedures as the Marotta valves. Initial tests show that the restrictors behave as specified. More tests will be conducted upon the arrival of special fittings for the restrictors.

GP-50 Pressure transducers (P1a, P1b, P3a, P3b) are under test.

A prototype of Box S has been constructed. It will be used to test flight components. The control electronic utilizes a Universal Slow Control Module (USCM), based on a successful

predecessor in AMS-01, to control gas transfer. The USCM is being built at Aachen III. Software controlling the gas mixing process and safety is being developed by MIT and Aachen-III.

The mechanical design and integration of the flight version proceeds in the AMS integration office at CERN in conjunction with Arde Inc. and NASA. The design, which has passed the first safety review on March 15 in Houston, is given in Figure 59.

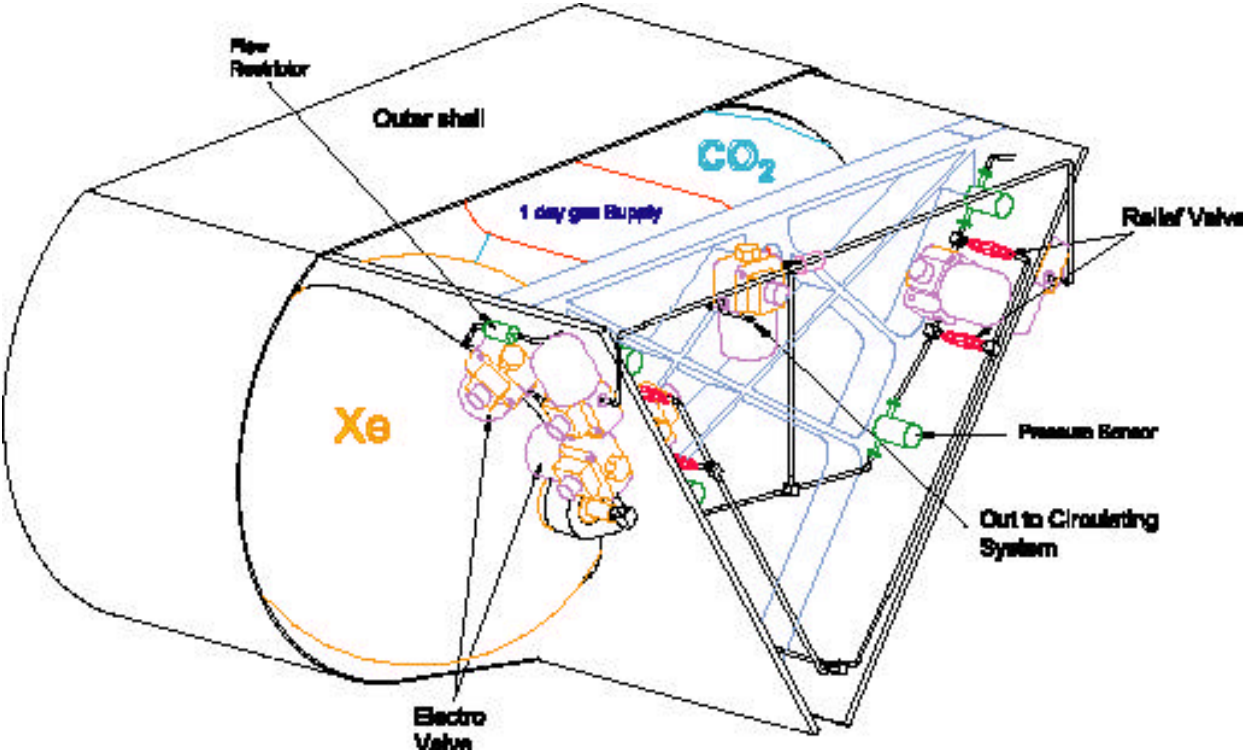


Figure 59: Box S as presented at the Safety Review on March 15, 2001 in Houston.

A Xenon recovery and storage system has been built at MIT. A cryogenic pumping system that is capable of extracting Xenon from the storage vessels and storing it in a removable bottle is under test. Preliminary testing of the pumping capacity indicates the system will be able to store the full Box S Xenon supply. The system also contains a residual gas analyzer for gas composition and contamination checks.

(iii) Manifolds

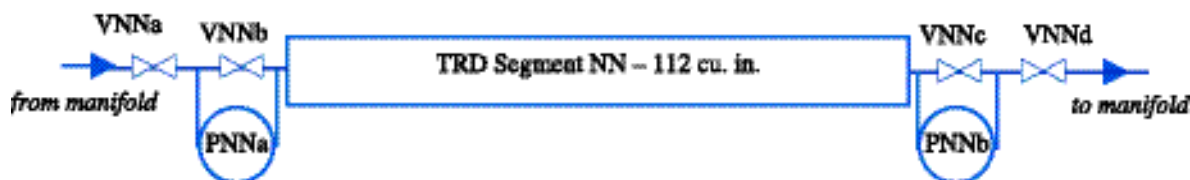


Figure 61 : One of 41 gas circuits, with isolation valves and pressure sensors on input and output (NN = 1 to 41).

From Box C, 6mm stainless steel gas lines run to the top rim of the TRD and to input and output manifolds. These manifolds are developed by MIT and interface to the TRD being built at Aachen. The 5248 tubes of the TRD are grouped into 41 segments composed of two towers of four 16 tube packages. The packages are connected in series to the manifolds to form 41 separate gas circuits, which can be isolated from the rest of the system by isolation valves on the input and output, as shown in Figure 61. The valves are doubled for redundancy. There are two (for redundancy) pressure sensors for each of the segments. 1.6mm o.d. CuNi tubing runs from the valves to the segments, where it is joined to PEEK tubing. Carbon fiber tubes around the sides of the TRD, which are attached to the top and bottom honeycomb panels, support the manifolds, the gas tubing and cables.

The isolation valves work in two modes. In case of a sudden pressure drop or power failure, the valves are closed automatically to prevent further gas loss. As a periodic check the valves may be closed and the pressure monitored to detect a slow leak.

The flipper valves (VNNa, VNNb, VNNc, VNNd) require a 100ms 12V, 1.5W, pulse to open or close. At other times they consume no power. The valves are positioned at the sides of the TRD in a region where the field is on the order of 100-200 Gauss. They will be enclosed in

magnetic shielding boxes in groups of five or six sets of valves. The boxes will also serve as leak protection for the valves.

Honeywell pressure sensors (PNNa, PNNb) are used. They operate at 10V, 25mW. They have been pressure tested. The flow resistance of the straw tube packages, valve assemblies and CuNi and stainless steel tubing of various diameters have been determined with an 80:20 Xe:CO₂ gas mixture. Special fittings have been constructed in Aachen to join 1.6 mm metal tubing with PEEK tubing.

Vibration testing of the valve and pressure sensor assemblies will be done in Aachen.

MIT has designed a prototype flight calibration tube that can be hermetically sealed and fulfills the NASA requirements concerning radiation sources in space. One of these tubes is being used by Box C for gain stability tests.

(iv) **Electronics for the TRD Gas System**

The control electronics for the gas system is shown in Figure 62.

The circuit boards UGSCsc and UGSCm provide an electronic interface between the Universal Slow Control Module (USCM) and the flight hardware and is the responsibility of INFN-Sezione di Roma . The USCM uses an addressing scheme for digital control at low power (mW) that controls interface electronics at high power (~W).

As seen in Figure 62, there are two parts to the TRD Gas System Slow Control that are represented as hatched boxes:

- **UGSCsc (Unit Gas System Control for boxes S and C)** Located in a crate near Box S or Box C, it will control their operations. It will shut the gas system down safely in case of power and communications failure to prevent overpressure.
- **UGSCm (Unit Gas System Control Manifold)** Controls and monitors the isolation valves, pressure sensors and temperature sensors of the TRD manifolds. It will be situated close to the TRD. It will control the flow of gas through the TRD modules and isolate any leaking segments.

TRD GAS SYSTEM SLOW CONTROL

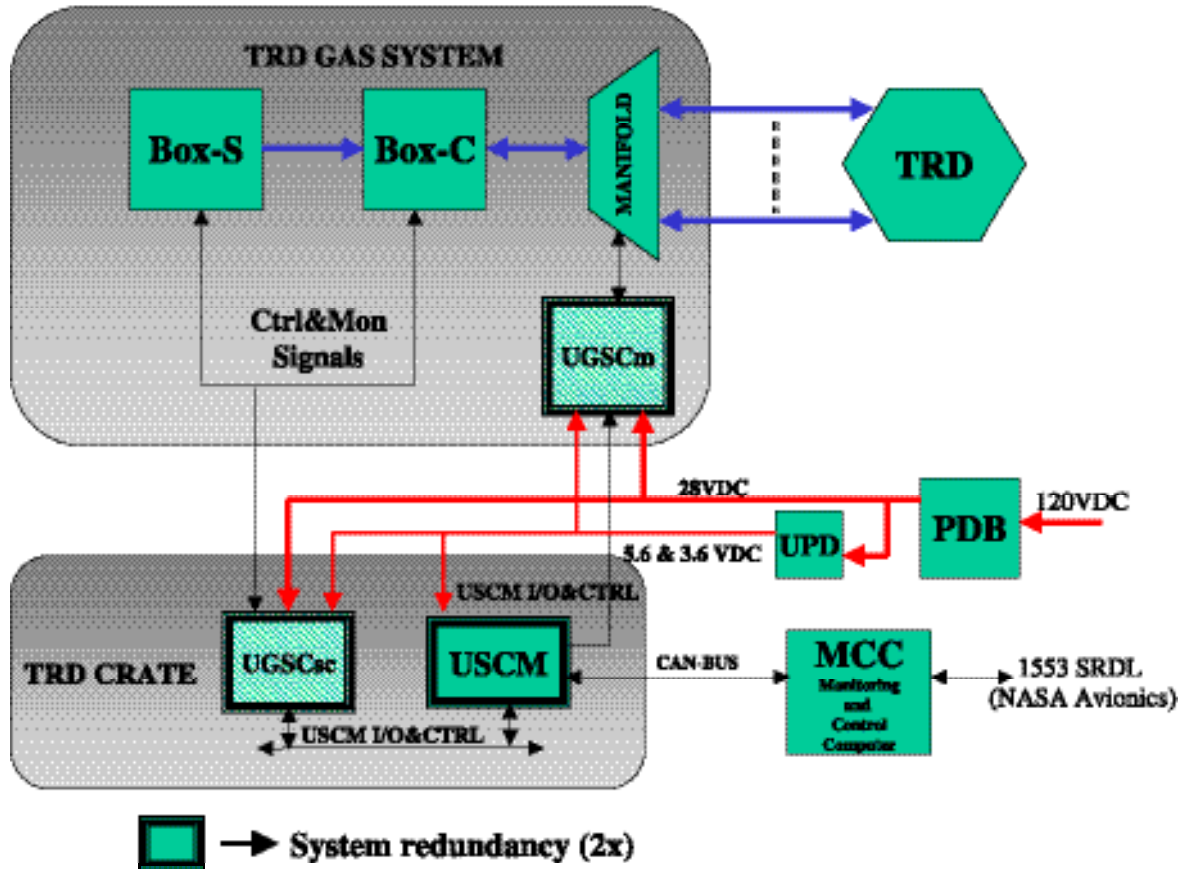


Figure 62: TRD gas system slow control

Both units are designed with redundancy and high reliability components. The USCM will transmit control signals and receive transducer data and alarms. Both are powered by a UPD (Unit Power Driver) that provides necessary voltage and current to operate valves, pumps, and the other parts of the TRD system.

(v) USCM Interface and Control Software

The USCM periodically reads out all data from all temperature and pressure sensors, the gas analyzer, valve status (open/close), etc. Thus, the USCM knows the complete status of the TRD gas system.

The USCM is connected to the Monitor and Control Computer (MCC) and Main DAQ Computers of AMS via CAN-bus (USCM I/O and control, Figure 62). The USCM contains the

monitoring program, which checks the status information of the gas system against pre-set conditions and executes commands. The conditions and commands are stored in the form of a decision table.

11) TRD Calibration in-situ

There are several factors that may affect TRD performance: uniformity of the tube geometry, the spread in the amplification factors of the electronic channels, the uniformity of the magnetic field across the TRD volume, and gas density fluctuations. Some of these factors (gas density variations and amplification coefficients of the electronic channels) are expected to vary during the flight and require in-situ calibration. Studies showed that e-p separation is not compromised if the uniformity of the TRD channels is 5% or better.

Two TRD calibration methods are under investigation: calibration with protons and random trigger calibrations in the South Atlantic Anomaly (SAA). A test setup has been built at CERN to simulate the performance of both calibration methods with a source.

Calibration with protons is based on analyzing the amplitude spectrum of protons recorded by AMS (Figure 63a and 52). The shape of the amplitude spectrum in a TRD tube is compared with the reference spectrum to extract an amplification factor corresponding to that tube. Corrections for temperature, track position inside the tube and proton momentum have been applied to extract the intrinsic tube gain factor.

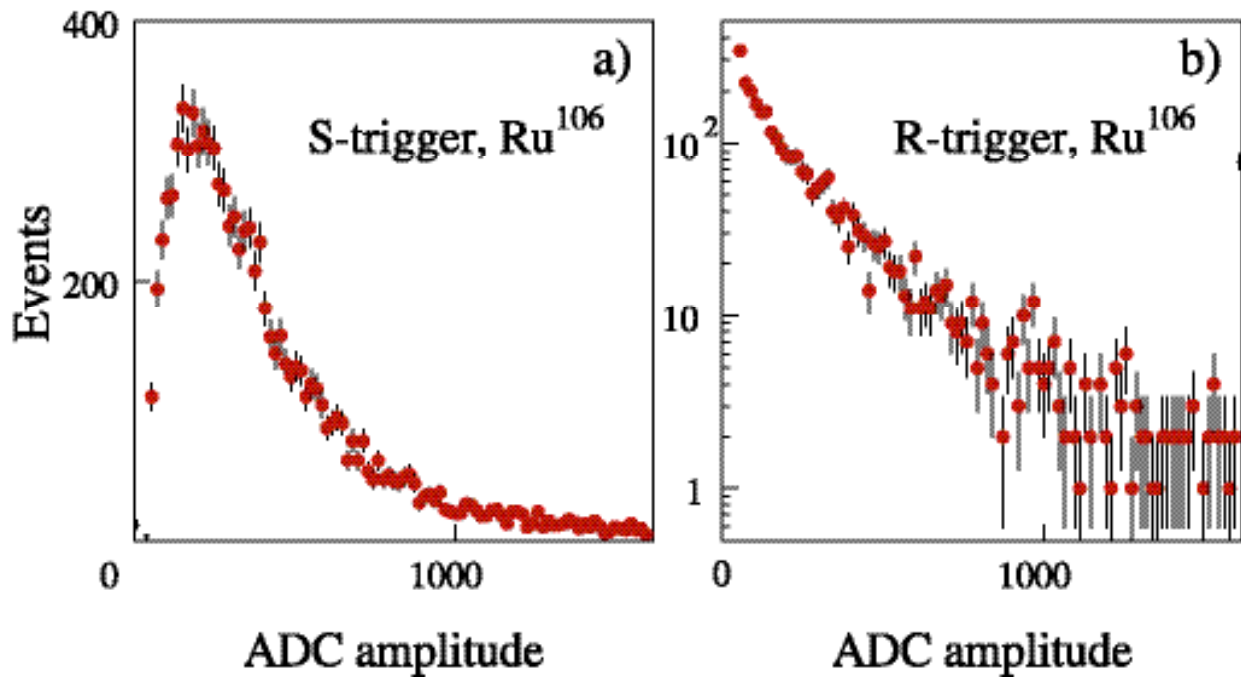


Figure 63: Single tube spectra for self-trigger and random trigger calibration

Random trigger calibration in SAA is based on analyzing a spectrum of random signals in the TRD. The flux of charged particles in SAA (most of these particles are protons of few hundred MeV) is comparable to the flux from a Ru^{106} source used for tests. This procedure does not require dedicated electronics. The gain fitting procedure is conceptually similar to that for calibration with protons.

Both procedures are feasible for use in the ISS, they provide similar precision of gain determination to about 3%. However, the time to achieve such accuracy is about 1 day for the proton calibration and about 10 min. for the random trigger calibration.

The construction of the TRD and the gas system is progressing well and we expect to test the entire system in the CERN test beam in 2002 in accordance with the construction plan shown in Table 9.

